AN EVOLUTIONARY APPROACH FOR SEMICONDUCTOR NANODEVICES OPTIMIZATION

FERNANDO CARVALHO DA SILVA. COELHO

AN EVOLUTIONARY APPROACH FOR SEMICONDUCTOR NANODEVICES OPTIMIZATION

Dissertação apresentada ao Programa de Pós-Graduação em Computer Science do Instituto de Ciências Exatas da Universidade Federal de Minas Gerais como requisito parcial para a obtenção do grau de Mestre em Computer Science.

Orientador: Omar Paranaiba Vilela Neto

Belo Horizonte

Fevereiro de 2014

FERNANDO CARVALHO DA SILVA. COELHO

AN EVOLUTIONARY APPROACH FOR SEMICONDUCTOR NANODEVICES OPTIMIZATION

Dissertation presented to the Graduate Program in Computer Science of the Universidade Federal de Minas Gerais in partial fulfillment of the requirements for the degree of Master in Computer Science.

Advisor: Omar Paranaiba Vilela Neto

Belo Horizonte

February 2014

Coelho, Fernando Carvalho da Silva.

C672e An Evolutionary approach for Semiconductor Nanodevices optimization / Fernando Carvalho da Silva. Coelho. — Belo Horizonte, 2014
xxviii, 69 f. : il. ; 29cm

Dissertação (mestrado) — Universidade Federal de Minas Gerais
Orientador: Omar Paranaiba Vilela Neto

1. Computação - Teses, 2. Nanotecnologia - Teses, 3. Computação evolucionária - Teses. I. Orientador. II. Título

CDU 519.6*82(043)

UNIVERSIDADE FEDERAL DE MINAS GERAIS
INSTITUTO DE CIÊNCIAS EXATAS
PROGRAMA DE PÓS-GRADUAÇÃO EM CIÊNCIA DA COMPUTAÇÃO

FOLHA DE APROVAÇÃO

An evolutionary approach for semiconductor nanodevices optimization

FERNANDO CARVALHO DA SILVA COELHO

Dissertação defendida e aprovada pela banca examinadora constituída pelos Senhores:

PROF. OMAR PARANAÍBA VILELA NETO - Orientador
Departamento de Ciência da Computação - UFMG

PROF. PAULO SÉRGIO SOARES GUIMARÃES
Departamento de Física - UFMG

PROF. THIAGO FERREIRA DE NORONHA
Departamento de Ciência da Computação - UFMG

Belo Horizonte, 21 de fevereiro de 2014.

Dedico esse trabalho a meus pais Angélica e Romildo que me apoiaram por todos esse anos de dedicação à minha formação.
Esses dois, me ensinaram o real valor de se enfrentar as dificuldades com sabedoria e a superá-las para atingir as vitórias que conquistamos por todos esses anos em nossa família.
Fica aqui também uma dedicação especial a todos os meus professores, desde o ensino fundamental, que sem dúvida, inflênciaram minha trajetória, até a escrita dessa dissertação.
Os grandes amigos, também não podem ser esquecidos, pois, esses lutaram juntos comigo, em todas as batalhas que enfrentamos, ao longo dos anos.

Agradecimentos

Aos professores do Departamento de Ciência da Computação, pela formação e apoio que me concederam ao longo desses anos de graduação e de mestrado.

Aos amigos do LECOM, pelas produtivas discussões no tempo em que estivemos juntos.

Aos amigos do grupo de computação gráfica, pelas ricas discussões e reuniões que tivemos.

Ao professor Paulo Sérgio e seu aluno, Juan Pablo, pelo auxílio nos trabalhos com cristais fotônicos.

Ao professor Eduardo Cotta, pelo simulador de microcavidades.

"Ninguém é digno do pódio se não usar os fracassos para conquistá-lo.
No one deserves a podium if they dont't take their failures to conquer it."
(Augusto Cury in Nunca desista dos seus sonhos)

Resumo

Uma das principais razões para o grande desenvolvimento computacional visto nas últimas décadas foi a miniaturização contínua no tamanho dos transistores. Contudo, estamos próximos do limite físico de miniaturização deste componente eletrônico. Portanto, com o intuito de manter o avanço do desempenho dos processadores, novas alternativas de materiais e tecnologias devem ser investigadas. A Nanocomputação visa o estudo de nanodispositivos e nanoestruturas para o desenvolvimento de uma nova geração de computadores, com arquiteturas inovadoras e eficientes. Dentre as possíveis soluções podemos destacar os nanodispositivos semicondutores. Neste trabalho investigaremos a otimização de dois tipos de nanodispositivos semicondutores diferentes, Cristais Fotônicos e Microcavidades, que podem permitir o desenvolvimento de uma futura geração de computadores que utilizam como variável de estado a luz ao invés da carga elétrica dos processadores convencionais.

Tipicamente, o processo de otimização destas estruturas físicas é empírico e lento, dependendo principalmente do conhecimento e intuição dos especialistas. A otimização mais robusta e eficiente exige a existência de modelos matemáticos e simuladores capazes de representar o comportamento estrutural dos dispositivos. Esses modelos podem assumir elevada complexidade computacional, tornando a avaliação sistemática dessas estruturas um desafio. Além disso, a busca por soluções eficientes esbarra em grandes espaços de busca e comportamento não linear. Desta forma, neste trabalho aplicamos algoritmos evolutivos na busca por soluções otimizadas que satisfaçam os requisitos necessários para o desenvolvimento de futuras aplicações.

Cristais fotônicos são sistemas cuja função dielétrica é periódica no espaço. Geral-

mente, essas estruturas são implementadas em um cristal semicondutor como, por exemplo, Arseneto de Gálio (AsGa), e possuem padrões de buracos preenchidas por ar. A partir da alteração dos parâmetros geométricos das cavidades do cristal, ou seja, geração controlada de defeitos na estrutura, a luz pode ter seu fluxo controlado, fato que permite o desenvolvimento de aplicações como portas lógicas ópticas, sensores de alta resolução, processamento quântico da informação, dentre outras. Neste projeto focamos na maximização do fator de qualidade da estrutura conhecida como L3, variando as posições geométricas e raios dos buracos ao redor do defeito. O fator de qualidade pode ser definido pela energia perdida por ciclo versus a energia armazenada no defeito. Os resultados obtidos em nossos estudos de caso superam aqueles previamente apresentados na literatura. Além disso, é importante destacar que a simulação de cada estrutura gerada é computacionalmente muito cara, o que levou ao desenvolvimento de um algoritmo distribuído e robusto que pudesse tirar proveito do maior número de computadores possíveis.
Já as microcavidades semicondutoras podem ser consideradas como cristais fotônicos de uma dimensão e são bases para uma variedade de dispositivos optoeletrônicos, tais como, lasers e diodos emissores de luz (LEDs), além de transistores óticos. Normalmente, estes materiais contém muitas camadas diferentes, cujas condições de crescimento devem ser altamente estáveis, com um controle preciso sobre a composição e espessura de cada camada individual. Contudo, incertezas durante o processo físico de crescimento fogem do controle dos especialistas e podem comprometer significativamente a eficiências dos dispositivos. Desta forma, neste projeto visamos não somente encontrar os parâmetros ideais que levem às soluções ótimas, mas também que garantam o crescimento de dispositivos robustos e eficientes. Este é o primeiro projeto que propõem a otimização da estrutura das microcavidades, principalmente focando em sua robustez. Diferentes tipos de microcavidades foram otimizadas e a estratégia proposta neste trabalho se mostrou eficaz, levando a estruturas com fator de qualidade maior que o descrito anteriormente na literatura e alta garantia de robustez no crescimento.

Palavras-chave: Algoritmo Evolutionário, Semicondutores, Microcavidades, Nanotecnologia, Nanodispositivos.

Abstract

Recently, one of the main reasons for the large computational development seen has been the continued miniaturization of transistors' size. However, the miniaturization of the electronic components is quickly approaching it's physical limits. Therefore, in order to maintain the advancement of processors' performance, there is the need of new alternative technologies and materials to be investigated. Thus, nanocomputing aims to study nanostructures and nanodevices for the development of a new generation of computers, with innovative and efficient architectures. Among the possible solutions we can highlight the semiconductor nanodevices. In this work it is investigated the optimization of two types of different semiconductor nanodevices: Photonic Crystals and Microcavities, that can enable the development of a future generation of computers that use light as a state instead of the electric charge applied in conventional processors.

In the last years, with the advances in the fields of computational intelligence and with the introduction of massive computing power, the design process has undergone a huge advance in optimizing structures and design in science and enginnering, where the optimization process is an essential part towards increasing quality, improving functionality and robustness of devices.

Typically, the process of optimizing these physical structures is empirical and slow, demanding knowledge and intuition of experts. A robust and efficient optimization requires the existence of mathematical models and simulators able to represent the devices' structural behavior. These models, in many cases, hold high computational complexity, delivering a scenario where systematic evaluation of these structures is a challenge. Moreover, the search for efficient solutions has to deal with large search spaces and nonlinear behavior. Thus, in this work it is

applied an evolutionary approach in the search for optimized solutions satisfying the requirements for the development of future applications' solutions.

Photonic crystals are systems whose dielectric function is periodic in space. Generally, these structures are implemented in a semiconductor crystal, for example, Gallium Arsenide (GaAs), and have patterns of holes filled by air. By changing geometrical parameters of the cavities of the crystal, that is, controlled generation of defects in the structure, the light can be controlled, a fact that allows the development of applications such as optical logic gates, high resolution sensors, quantum processing information, among others. In this project the focus is on maximizing the Quality Factor of a structure known as *L3*, by varying the geometric positions and radii of the holes around the defect. The results obtained in our case studies outnumber those previously presented in the literature. Furthermore, it is important to note that the simulation of each structure generated is computationally very expensive, which led to the development of a massively distributed and robust algorithm that could take advantage of the largest possible number of computers.

In the other study case, semiconductor microcavities, which can be considered as a 1-dimension photonic crystal, are the bases for a variety of optoelectronic devices such as lasers and light emitting diodes (LEDs), and optical transistors. Typically, these materials contain many different layers, whose growth conditions should be highly stable, with precise control over the composition and thickness of each individual layer. However, uncertainties in the physical process of growth beyond the control of experts can significantly compromise the efficiency of the final device. Thus, in this project it is a goal to not only find the optimal parameters that lead to optimal solutions, but also to ensure the growth of robust and efficient devices. This is the first project proposed to optimize microcavities' structure, mainly focusing on its robustness. Different types of microcavities were optimized and the strategy proposed in this study proved to be effective, leading to structures with higher Quality Factor than previously described in the literature while delivering robustness in the growth process.

List of Figures

List of Tables

List of Acronyms

PCMDGA Photonic Crystal Massively Distributed Genetic Algorithm

MCGA Microcavity Genetic Algorithm

Contents

Chapter 1

Introduction

1.1 Motivation

The interest in Nanoscience and Nanotechnology has emerged due to the possibility of developing novel materials with improved and innovative properties. According to scientists, nanotechnology will be able to change the nature of almost everything already done, which should impact areas such as medicine, engineering, telecommunications, energy and computing. This is a truly multidisciplinary area, involving scientists from different fields of knowledge such as chemistry, physics, engineering, computer science, biology and medicine.

The advance in Nanoscience and Nanotechnology is allied to the development of computational models of biological, chemical and physical systems, which allow researches to simulate novel nanomaterials, devices and applications. Particularly, the large computational development seen in last years has been provided by the continued miniaturization of transistors' size. However, the miniaturization of the electronic components is quickly approaching it's physical limits. Therefore, in order to maintain the advancement of processors' performance, there is the need of new alternative technologies and materials to be investigated. In this way, studying nanostructures and nanodevices for the development of a new generation of computers, with innovative and efficient architectures, is a thriving path towards filling this demand. Among the possible solutions, the semiconductor nanodevices, can be highlighted.

These systems, when empowered by the advances in the fields of intelligent computing paradigm and with the introduction of massive computing power, have facilitated a move away from simple analytical systems towards large scale intelligent computer-aided design optimization.

Optimization is an essential part of research, both in science and in engineering. In many cases, the research goal is an outcome of an optimization problem, for example, designing aerodynamics shapes [Giannakoglou, 2002], space mission design [Croisard et al., 2010] or improving quality of photonic systems [Saucer and Sih, 2013].

Typically, the process of optimizing these physical structures is empirical and slow, demanding knowledge and intuition of experts. A robust and efficient optimization requires the existence of mathematical models and simulators able to represent the devices' structural behaviour. These models, in many cases, hold high computational complexity, delivering a scenario where systematic evaluation of these structures is unfeasible. Moreover, the search for efficient solutions has to deal with large search spaces and nonlinear behaviour which is a challenging problem which are known as '*expensive optimization problems*'.

In the search of these promising properties found in the nanoscale, this work investigate the optimization of two types of different semiconductor nanodevices: Photonic Crystals and Microcavities, that can enable the development of a future generation of computers that uses light as a state variable instead of the electric charge applied in conventional processors.

Photonic crystals are systems whose dielectric function is periodic in space. Generally, these structures are implemented in a semiconductor crystal, for example, Gallium Arsenide (GaAs), and have patterns of holes filled by air. By changing geometrical parameters of the cavities of the crystal, that is, controlled generation of defects in the structure, the light can be controlled, a fact that allows the development of applications such as optical logic gates, high resolution sensors, quantum processing information, among others.

In the other study case, semiconductor microcavities, which can be considered as an 1-dimension photonic crystal, are the bases for a variety of optoelectronic devices such as lasers and light emitting diodes (LEDs), and optical transistors.

1.2 Goals

In the search for the optimal photonic crystal and microcavity structure, this work aims to study and apply an evolutionary approach tailored to each study case, satisfying the requirements for the development of future applications' solutions. Thus, this project has two distinct optimization targets: the photonic crystals and microcavities structures.

For photonic crystals, the focus is on maximizing the Quality Factor, Q, of a structure known as *L3*, by varying the geometric positions and radii of the holes around the defect, in order to find Q higher than that previously presented in the literature.

On the other hand, in the case of microcavities, typically, these materials contain many different layers, whose growth conditions should be highly stable, with precise control over the composition and thickness of each individual layer. However, uncertainties in the physical process of growth beyond the control of experts can significantly compromise the efficiency of the final device. Thus, in this project it is a goal to not only find the optimal parameters that lead to optimal solutions, but also to ensure the growth of robust and efficient devices.

1.3 Contributions

From the photonic crystals cavities optimization, the results obtained in our case studies outnumber those previously presented in the literature. Furthermore, it is important to note that the simulation of each structure generated is computationally very expensive, which led to the development of a massively distributed and robust algorithm that could take advantage of the largest possible number of computers.

Simultaneously, to the best of our knowledge this is the first project proposing the optimizations of microcavities' structure, mainly focusing on its robustness. Different types of microcavities were optimized and the strategy proposed in this study proved to be effective, leading to structures with higher Quality Factor than those previously described in literature while delivering robustness in the growth process.

1.4 Roadmap

In chapter 2 there is a background discussion about what are semiconductors, microcavities, Photonic Crystals and Evolutionary Algorithms in order to aid readers from different backgrounds to better understand the overall work.

To discuss previous work on optimization of real world structures, chapter 3 investigates the current literature to grab the state of art in the area where this work innovates: optimization of nanodevices, and parallel evolutionary algorithms.

Chapter 4 does a deep discussion on the methods used to optimize each study case.

Finally, chapter 5 reveals the outcome of the optimization process for both: photonic crystals and microcavities structures.

Chapter 2

Background

The study of semiconductors nanodevices optimization is a multidisciplinary area which comprises concepts of matter's structure and computer science, so, in order to better understand this work, this section gives an introduction to what are Semiconductors, Photonic Crystals, Microcavities and Evolutionary Algorithms and how they work.

2.1 Semiconductor

Semiconductors are materials in which electrical conductivity can change depending from the conditions that the material is exposed, so it can behave like an insulator or a conductor.

As shown in figure 2.1 (a) an insulator is a material in which the last band, with electrons, is completely filled, so that an eletrical field applied to it is not able to change electrons momentum. On the other hand, conductors, as represented in figure 2.1 (b), have their last band, with electrons, partially filled and an eletrical field can put electrons in movement, thus, allowing conduction.

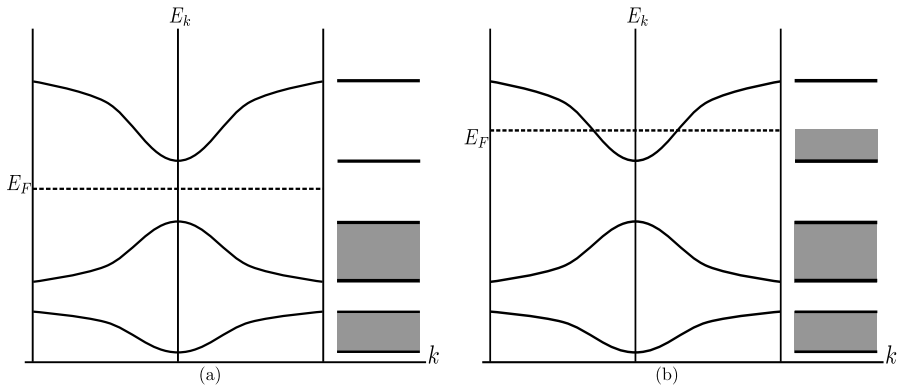

Figure 2.1: Band occupation in insulators (a) and conductors (b). Shaded regions represents the occupation of bands by electrons. [Rezende, 2004]

In an insulating crystal, only at temperature $T = 0K$ the last band, called the valence band is completely filled. When the temperature is higher than zero, valence band electrons can gain enough thermal energy to reach the next band, called conduction band, which was empty at $T = 0$. The migration of electrons to the conduction band leaves, in the valence band, states that behave such as positive charge carriers, called holes. The electrons in the conduction band and holes in the valence band produce electrical current under the action of an external field. The conductivity of the material depends on the number of electrons that passes into the conduction band, which can be calculated probabilistically. This amount of electrons is proportinal to the temperature and the inverse of the energy gap between the two bands. This energy is represented by E_g, where g is the gap index. The materials which are insulators at $T = 0K$, but have an E_g relatively small, on the order of $1eV$ or less at room temperature, have significant conductivity and, therefore, are called semiconductors. Figure 2.2 shows the occupation of the valence and conduction bands in a semiconductor. In these materials the number of electrons in the conduction band can be higher in relation to an insulator, but is still much less than the number of free electrons in a metal. Therefore, the conductivity of the semiconductor is much smaller than that of metals. The main difference between an insulator and a semiconductor is the value of E_g. For example, silicon has $E_g = 1.1eV$ and is a semiconductor, while diamond which has the same structure of Si, but comprised of atoms of C has $E_g = 5eV$, and behaves as a good insulator. The Silicon Oxide, $Si0_2$, have an $E_g \simeq 8eV$ and is

also an insulator. The difference in the values of E_g may not seem so great to produce radical change in conductivity, however, the occupation of the conduction band decreases exponentially with the increase of the $\frac{E_g}{k_B T}$ ratio, as described in [Rezende, 2004].

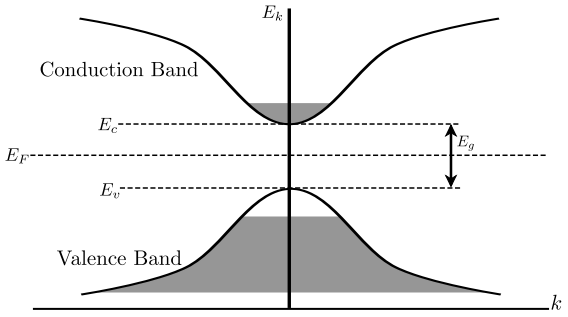

Figure 2.2: Conduction and valence bands in semiconductors. Shaded regions represents electrons ocupation in $T > 0$. The distance between bands is the energy gap E_g. [Rezende, 2004]

2.2 Microcavities

A microcavity is a system in which a light emitting material can interact with at most a single cavity-resonant-mode or there are no interactive electromagnetic modes permitted to interact within the material transition width. Thus, enhanced or suppressed spontaneous emission can be seen in this system, and in a very high cavity quality factor Q, even oscillatory spontaneous emission is induced [Morin et al., 1992; Raimond et al., 2001].

Semiconductor microcavities have been applied in important studies of various areas for technological and purely scientific purposes. Among the several studies performed in microcavities we can emphasize: (a) the development of low threshold emission lasers, since the microcavities acts as laser without population inversion [Imamōglu and Ram, 1994]; (b) construction of optical transistors [Cotta, 2009] and other all optical devices [De Matos et al., 2000]; (c) a parametric generator of twin photons through the parametric up- or down-conversion process [Ma et al., 2011; Banaee and Young, 2008]; (d) the Bose-Einstein condensate of exiton-polaritons [Kasprzak et al., 2006]; (e) effects of optical bistability fully con-

trollable [Cotta and Matinaga, 2007], among many others. All these phenomena and devices require an excellent coupling between the resonance cavity and the gain medium, which mainly consist of quantum-well(s) or quantum-dots. Thus, it is very important to find an exact coupling between the cavity-resonance and the emission peak of the gain media. Therefore, beyond an architectural design project, a precise control of the growth becomes essential to take advantage from the optical properties of the sample materials.

In a typical sample, a gain medium is placed at antinode of a λ cavity formed by two Diffracted Bragg Reflector (DBR) mirrors and kept at $10K$ in a cold finger cryostat. The sample is grown by Molecular Beam Epitaxy technique (MBE), that rotates during growth of the DBR mirrors and the gain medium, but stopped at a specific angle for growing the spacer layer, generating a thickness gradient across the sample. This process allows making a cavity-detuning when excites the sample in different positions on the surface. The Quality Factor of the cavity is measured directly using an unpolarized white light source, focusing normally on the sample surface.

Figure 2.3 shows the structure's schematic form of a microcavity. In this figure we can see that the heterostructure is grown on top of a Gallium Arsenite ($GaAs$) substrate oriented in the direction [100]. On the substrate is deposited alternating layers of two different materials based on a ternary alloy of $Al_xGa_{1-x}As$, where x is the concentration of Aluminum. The deposition of the first two layers gives rise to the pair that is presented in the figure by white (refractive index n_1 and thickness l_1) and light gray (refractive index n_2 and thickness l_2). The periodic superposition of pairs of layers N_1 times forms a DBR mirror (Distributed Bragg Reflector) at the bottom of the sample and an upper DBR mirror with N_2 pairs of layers. The two DBR mirrors are separated by a spacer layer (refractive index n_3 and thickness l_3) also of $Al_xGa_{1-x}As$, forming a Fabry-Perot type cavity. In the middle of the cavity is placed a quantum well (SQW) of GaAs 10nm thick [da Cunha, 2011; Coelho et al., 2013].

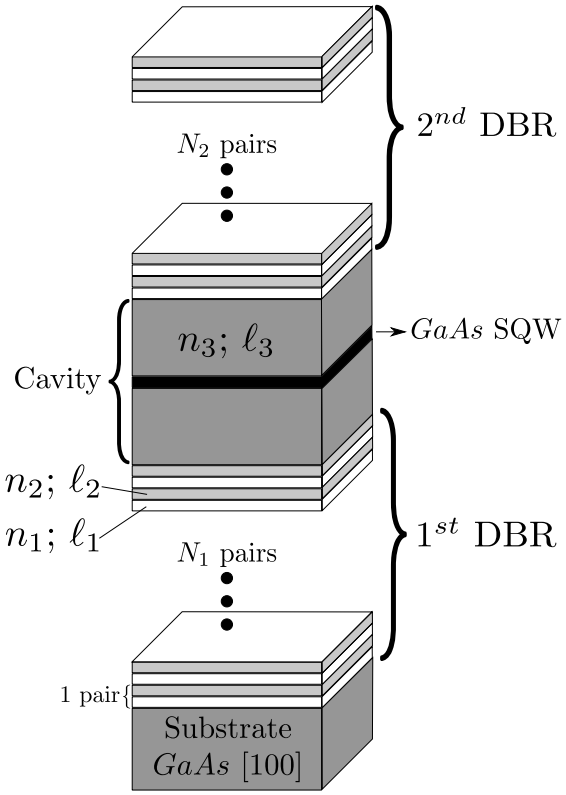

Figure 2.3: Microcavity's structure

2.3 Photonic Crystals

A crystal is a periodic arrangement of atoms or molecules. The pattern with which the atoms or molecules are repeated in space is the crystal lattice. The crystal presents a periodic potential to an electron propagating through it, and both the constituents of the crystal and the geometry of the lattice dictate the conduction properties of the crystal. [Joannopoulos et al., 2011]

The theory of quantum mechanics in a periodic potential explains that electrons propagate as waves, and waves that meet certain criteria can travel through a periodic potential without scattering (although they will be scattered by defects and impurities). [Joannopoulos et al., 2011]

Importantly, however, the lattice can also prohibit the propagation of certain waves. There may be gaps in the energy band structure of the crystal, meaning that electrons are forbidden to propagate with certain energies in certain direc-

tions. If the lattice potential is strong enough, the gap can extend to cover all possible propagation directions, resulting in a complete band gap. For example, a semiconductor has a complete band gap between the valence and conduction energy bands, as shown in section 2.1.[Joannopoulos et al., 2011]

The optical analogue is the photonic crystal, in which the atoms or molecules are replaced by macroscopic media with differing dielectric constants, and the periodic potential is replaced by a periodic dielectric function (or, equivalently, a periodic index of refraction). If the dielectric constants of the materials in the crystal are sufficiently different, and if the absorption of light by the materials is minimal, then the refractions and reflections of light from all of the various interfaces can produce many of the same phenomena for photons (light modes) that the atomic potential produces for electrons. One solution to the problem of optical control and manipulation is thus a photonic crystal, a low-loss periodic dielectric medium. In particular, we can design and construct photonic crystals with photonic band gaps, preventing light from propagating in certain directions with specified frequencies (i.e., a certain range of wavelengths, or "colors," of light). Photonic crystal can, also, allow propagation in anomalous and useful ways, which is a property that gives these strutures promissing applications. [Joannopoulos et al., 2011]

In figure 2.4 there is an example of a photonic crystal with the "L3" defect, which was the first type of photonic crystal nanocavity in which quality factors in excess of 10^4 were obtained experimentally [Chalcraft et al., 2007].

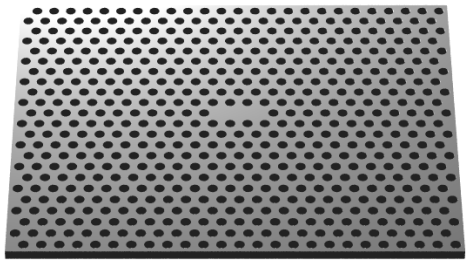

Figure 2.4: L3 defect in Photonic Crystal lattice, shown in perspective. [Akahane et al., 2005]

The "L3" defect is built by removing three holes from the photonic crystal hexagonal lattice ([Fan et al., 2011]), as shown in figure 2.5. In this lattice, all holes origin are equally distant by one unit and the distance between two rows is $sin(\frac{\pi}{3})$.

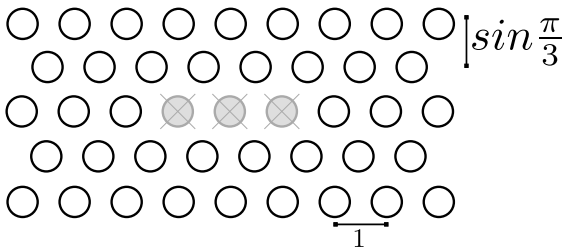

Figure 2.5: Schematic of how the L3 defect in Photonic crystal lattice is built.

[Akahane et al., 2003] defined that the Quality factor, Q, of a cavity is determined by the energy loss per cycle versus the energy stored. With no absorption by the cavity material, Q is determined by the reflection loss at the interface between the interior and exterior of the cavity.

In [Akahane et al., 2005] and [Chalcraft et al., 2007], it has been shown theoretically and experimentally that by changing the geometry of the holes surrounding the "L3" defect, cavities' quality factor can be broadly increased.

One application of a photonic crystal, that describes how it works, is to determine the refraction index of liquid solutions. The basic idea is to immerse the crystal in the sample and the induced change in the background refractive index produces a shift in the resonance frequency of the cavity mode, this shift can be used to characterize the sample. Since the Q factor is inversely proportional to the width of the transmission peak, the detection limit of such sensors is determined by the quality factor of the cavity. In this way, a higher Q produces a high precision sensor. [Pablo Vasco Cano, 2013]

These photonic cavities have many applications in enginnering and science. Among these applications, we find high-resolutions sensors [Scherer et al., 2006], quantum information processing [Michler et al., 2000] and the development of logic gates [Noshad et al., 2012].

2.4 Evolutionary Algorithms

Evolutionary Algorithms are general purpose optimization tools, designed to search in non-linear function spaces. These algorithms are based in the species evolution principle, where the most fitted individuals survive. In this way, an individual in a population, represents potential solutions to a problem, in which each individual holds a codification whose fitness can be evaluated by a mathematical function. These populations can be genetically mutated through generations, and it's individuals strives to survive in an procedure that seeks to choose the most fitted. After a number of generations, a convergence of solutions can be observed around the best individual.

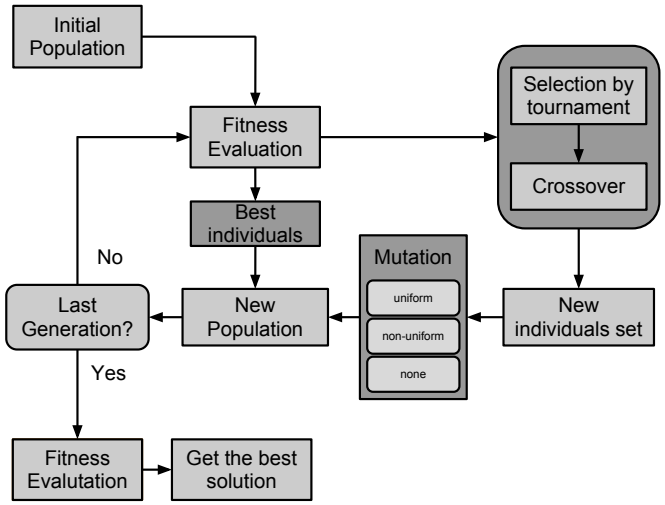

Figure 2.6: An evolutionary algorithm schema

Traditionally, a generation based Evolutionary Algorithm, as shown in figure 2.6, maintains a potential solutions population, encoded as an array of values representing function parameters being optimized. Initially, the group of potential solutions is determined randomly. These potential solutions, named individuals, are allowed to evolve over a number of generations. At every generation, the fitness of each potential solution is calculated. The fitness is a measure of how well the potential solution optimizes the objective function. The subsequent generation is created by recombining pairs of chromosomes in the current generation.

Recombination between two chromosomes is the method through which the populations "evolve" better solutions. The solutions are probabilistically chosen for recombination based upon their fitness. The "children" chromosomes produced by the genetic recombination are not necessarily better than their parental chromosomes. Nevertheless, because of selective pressure applied through a number of generations, the overall trend is toward better solutions [Baluja, 1992].

Chapter 3

Related work

The advances in the fields of computational intelligence paradigm and the introduction of massive computing power have facilitated a move away from paper-based analytical systems towards digital models and computer simulations. In this way, the use of these models has allowed the development of a class of problems known as "expensive optimization problems", as discussed in [Goh and Tenne, 2010], which are problems with high computational cost, whose complexity can arise due to:

- Resource-intensive evaluations of the objective function, when a computer simulation replaces a real-world laboratory experiment during the optimization process. Such simulations can be prohibitory expensive, requiring from minutes to many hours of evaluation time for each candidate solution.
- Very high dimensional problems when there are multiple variables implying in a huge search space. This scenario can deliver an intractability of the optimum solution.

Dispite the challenges, computer-aided design optimization, using an evolutionary approach, has now involved a wide range of design applications, which includes the design of aerodynamic shapes [Giannakoglou, 2002], super-capacitors fuel-cell hybrid electric vehicle optimization [Paladini et al., 2007], preliminary space mission design under uncertainty [Croisard et al., 2010] and photonic crystals systems as will be discussed in section 3.1.

3.1 Optimization in Photonic Crystals

As discussed in [Jiang et al., 2003], the optimization process of photonic components in which the minimum feature size is of the order of a wavelength or smaller poses significant computational challenges because of the need for rigorous solution of Maxwell's equations with computationally intensive numerical tools such as the finite-difference time-domain (FDTD) method, whose implementation can be found in tools such as MEEP [Oskooi et al., 2010].

Photonic crystal and compact waveguide structures are examples of devices that are often designed by manual scanning of desired performance metrics as a function of device parameters. This approach not only can become time consuming but also can leave the device not fully optimized and overlook novel, unanticipated solutions. [Jiang et al., 2003]

Therefore, many papers have been published regarding the optimization of geometric features of a photonic crystal, in order to improve a desired property of these structures.

[Sanchis et al., 2004] has used a genetic algorithm to reliably determine the optimized photonic-crystal-based structure for a spot size converter.

[Ye et al., 2004] has used an evolutionary approach to design a two-dimensional anisotropic photonic crystal of square lattice with a maximal absolute band gap. The unit cell is divided equally into many small squares, and each filling pattern of squares with two dielectric materials corresponds to a binary number.

In [Akahane et al., 2005], a photonic nanocavity with a high Q factor of 100,000 and a modal volume V of 0.71 cubic wavelengths, is demonstrated. This result, was achieved by further improving a point-defect cavity in a two-dimensional photonic crystal slab, where the arrangement of six air holes in the L3 cavity's line was fine-tuned.

A genetic algorithm was used in [Håkansson et al., 2005] to design the optimum configuration of defects that when put within a photonic-crystal taper improves the coupling efficiency between dielectric and photonic crystals waveguides.

[Quan et al., 2010], propose and experimentally demonstrate a deterministic method to design an ultrahigh Q, wavelength-scale photonic crystal nanobeam cavity that is strongly coupled to the feeding waveguide. The design approach is

deterministic in the sense that it does not involve any trial-based hole shifting, resizing and overall cavity rescaling to ensure the ultrahigh Q-factor of the cavity.

[Quan and Loncar, 2011] extends the previous work by demonstrating designs of dielectric-mode and air-mode cavities with $Q > 10^9$.

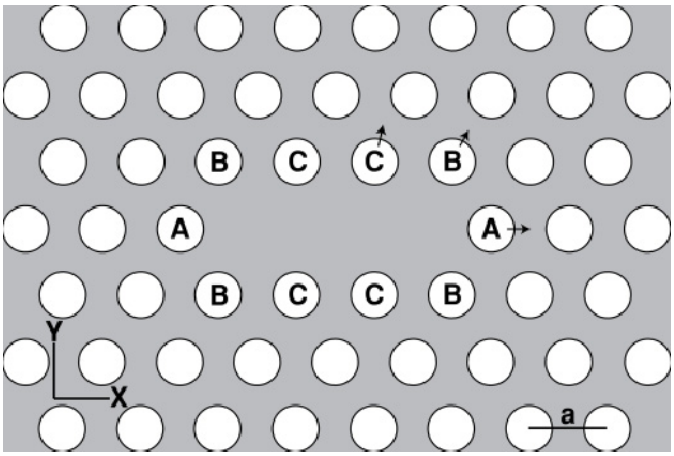

Figure 3.1: Holes shifted by [Saucer and Sih, 2013]

[Saucer and Sih, 2013] by slightly shifting the holes on the edge of the L3 cavity, as shown in figure 3.1, has achieved an cavity whose the quality factor, Q, is 567,000, by applying a gravitational search algorithm.

In this work, a massively distributed genetic algorithm is applied to optimize photonic cavities, overcomming the expensive process of evaluating the many individuals needed by the evolutionary process.

3.2 Microcavities optimization

In literature, to the best of our knowledge, there is no work optimizing photonic microcavities synthesis process, such as have been done in this work.

3.3 Parallel Evolutionary Algorithms

As discussed in [Desell et al., 2010], these complex models, such as those pointed in the beginning of this chapter, have many local optima and evolutionary algorithms

are very useful for quickly finding solutions in these challenging search spaces. In addition to the complex search spaces involved, calculating the objective function can be extremely demanding computationally. Because of this, distributed computation is a necessity. In order to address these computational demands, top-end distributed computing systems are surpassing hundreds of thousands of computing hosts; and as in the case of Internet based volunteer computing systems, they can also be highly heterogeneous and faulty.

Generally, as pointed by [Desell et al., 2010], distributed evolutionary approaches can be:

- Sequential, where new populations are generated sequentially and individuals are evaluated in parallel.
- Hybrid, where there are islands of populations and individuals in these islands are evaluated in parallel, and then an asynchronous migration happens due to a certain criteria.
- Asynchronous, where there is a single-population and individuals are generated at the demand of an evaluating client and then, their results are send back to a central hub to be integrated in the main population.

Typical applications of Evolutionary Algorithms require large scale computing resources which are derived from inherently complex fitness evaluation functions, large numbers of individuals per generation, and the number of iterations required by EAs to converge towards a satisfactory solution. Therefore, any source of computing power can significantly benefit researchers using evolutionary algorithms. So, the use of volunteer computing as a platform for harnessing the computing resources of commodity machines that are nowadays present at homes, companies and institutions can be used to improve these evolutionary process. Taking into account that currently desktop machines feature significant computing resources volunteer computing has become a cost-effective platform for running time consuming evolutionary algorithms in order to solve complex problems, such as finding substructure in the Milky Way Galaxy, as presented in [Cole et al., 2010], as a great example of the asynchronous approach for evolutionary algorithms.

Other works, also leverage the use of massively distributed algorithms to solve the challenge of evolving problems whose fitness evaluations are complex: [Laredo et al., 2010] discuss the use of scalable peer-to-peer evolutionary algorithm and [Tantar et al., 2008] propose a grid-based genetic algorithm combined with an adaptive simulated annealing for protein structure prediction.

On the other hand, there are many works regarding several models that have been used for fitness approximation to overcome the huge time required to evaluate individuals. [Jin, 2005] describes the most popular ones, which are polynomials (often known as response surface methodology), the kriging model, most popular in design and analysis of computer experiments (DACE), the feedforward neural networks, including multi-layer perceptrons and radial-basis-function networks and the support vector machines.

Chapter 4

Methodology

In this work there are two optimization models, one for each application studied: Microcavities and Photonic Crystals. These models can be optimized by a myriad of different optimization techniques. Due to time constraints, this work has focused in applying two different Evolutionary Algorithm approaches designed to each study case.

Section 4.1 describes how the Evolutionary Algorithm applyied in this work was set up for optimizing the models proposed.

Section 4.2, discusses about the process used to optimize the L3 photonic crystal cavity using the Photonic Crystal Massively Distributed Genetic Algorithm (PCMDGA), in order to overcome the computational complexity of evaluating each candidate solution generated by the developed algorithm.

Section 4.3, leverages discussion about how microcavities were optimized to achieve robust and high quality designs, using a typical Genetic Algorithm, namely Microcavities Genetic Algorithm (MCGA).

4.1 Optimization algorithm

For optimizing the strutures studied, in this work, it has been applied an Evolutionary Algorithm as introduced in section 2.4.

The Algorithm, initially, creates a set of randomly generated individuals to compose the initial population.

Individuals are, then, selected based in their fitness to create couples and have their genes crossed to generate new individuals. Thus, each couple selected perform the crossover procedure where each gene for each son is computed according to

$$\begin{aligned} Son_1 &= R * Parent_1 + (1 - R) * Parent_2 \\ Son_2 &= (1 - R) * Parent_1 + R * Parent_2 \end{aligned} \tag{4.1}$$

where R is a random value between 0 and 1.

This crossover is always performed when new individuals are needed to create a new population. In order to broaden the search, these new individuals generated are randomly chosen to perform mutation. In the mutation process, genes are chosen to receive a new values. It has been applied, in this work, three kinds of mutation: uniform mutation, non-uniform mutation and side-shift mutation.

Elitism is ensured by always copying a number of best individuals from the last generation to the current generation.

4.1.0.1 Non-uniform mutation

Non-uniform mutation, as described in [Michalewicz, 1996], is a technique to make a fine search and ensure that at least a local optimum is reached. So a gene v is selected through a mutation rate, and then applying equation 4.2 to compute the new value.

$$v' = \begin{cases} v + \Delta(t, UB - v) & \text{if random value 0} \\ v - \Delta(t, v - LB) & \text{if random value 1} \end{cases} \tag{4.2}$$

where LB and UB are lower and upper domain bounds for variable v. t represents the generation number. The function $\Delta(t, y)$, described in equation 4.3 returns a value in the range $[0, y]$ that rapidly approaches 0 as the end of generations draws near. In this way, we allow our search to spread in the space initially and very locally at later stages; thus tunning the search to minor steps, which brings benefits when minimum and maximum can be very near on the search space. When the algorithm has no generations, the criteria can be randonly chosen during the evolution to determine when fine search will be held.

$$\Delta(t, y) = y.(1 - r^{(1-\frac{t}{\tau})^b}) \tag{4.3}$$

In equation 4.3, t is the current generation, y is the maximum value that the function can return, r is a random number from [0..1], τ is the maximal generation number, and b is a system parameter determining the strengh of the shift that is going to happen in the gene.

4.2 Optimizing L3 Photonic Cavities

4.2.1 Problem definition

In this work, the "L3" photonic cavity, described in section 2.3, has been modeled for optimization by varying the geometric parameters of the holes surrounding the cavity, in order to find the best possible Quality Factor, Q.

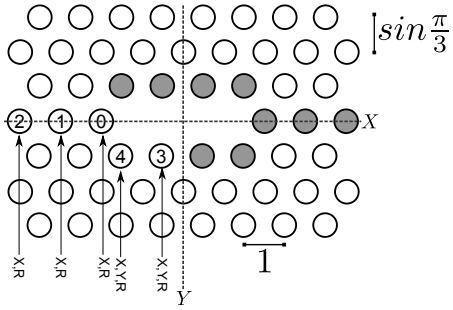

Figure 4.1: Photonic Crystal optimization schema

Figure 4.1 illustrates the setup used in this work for the optimization. The holes 0, 1 and 2 can move in the X axis in both directions and their radius can grow or shrink. Meanwhile, holes 3 and 4 can move freely in X and Y axis and the radius can also grow or shrink. Therefore, in table 4.1 there is a description about how the holes can change their parameters whose range were arbitrarily chosen to reduce overlapping probability among holes. All values are relative to their holes original position and size.

In this way, to reduce computational complexity, all the changes done to any hole are mirrored in the X and Y axis, changing the gray holes, so that the crystal

is symmetrical in both axis.

In order to simplify the optimization process all variables are limited to real numbers ranging from 0 to 1 which are latter interpolated to match cavities' attributes, as described in table 4.1.

Hole ID	Attribute	Attribute range
0, 1, 2	x	(-0.4, 0.4)
	radius	(50%, 150%)
3, 4	x	(-0.4, 0.4)
	y	(-0.4, 0.4)
	radius	(50%, 150%)

Table 4.1: Description of parameters range relative to the original hole location and size, as shown in figure 4.1, in units relative crystal's lattice parameter a.

For evaluating the Photonic Crystal's Quality Factor, Q, the MEEP simulator was applied [Oskooi et al., 2010], which is a free Finite-Difference Time-Domain (FDTD) simulation software package, developed at MIT, to model electromagnetic systems.

Hence, a script containing informations about crystal's slab geometric configuration and light's excitation center, frequency and pulse's width are delivered to MEEP for evalution, whose result is shown in figure 4.2.

```
mode_volume: 1500.0, 5.75783862536483, 6.27681289869532, 0.917318823787409
harminv0:, frequency, imag. freq., Q, |amp|, amplitude, error
harminv0:, 0.2572772, -3.507373e-4, 366.7661601, 0.0381568, 0.008255704-0.037252761i, 5.41484e-6
harminv0:, 0.2582758, -2.656415e-4, 486.1361768, 0.0069656, -0.00178357+0.006733453i, 1.52452e-5
harminv0:, 0.2634840, -4.955667e-8, 258411.482, 0.52534709, 0.023372491+0.524826922i, 1.13022e-8
run 0 finished at t = 1500.0 (60000 timesteps)
                                                  Quality factor

Elapsed run time = 3431.12 s
```

Figure 4.2: MEEP photonic crystal Quality Factor output

Each line with the string *harminv0* represents an excited mode, and each of them, holds a Quality Factor. Therefore, the crystal's quality factor is given by the greatest quality value, highlighted in the example in figure 4.2.

Thus, the optimization process goal is to find the highest possible Q, as shown in equation 4.4.

$$Solution = MAX(f(x_0, x_1, x_2, x_3, x_4, y_3, y_4, r_0, r_1, r_2, r_3, r_4)) \tag{4.4}$$

where f is the function that evaluates Q and x_n, y_n are the parameters for the horizontal and vertical moviment of holes and r_n is the radius of each hole.

4.2.2 Applied optimization algorithm

The Evolutionary Algorithm implemented here, works in the same way of traditional Genetic Algorithm, as described in section 4.1, however with individuals being replaced continually in a single population, instead of generations where all individuals not in the elitist set are replaced at once.

The process flow is shown in figure 4.3. Thus, the Genetic Algorithm generates new individuals based on population's current state in response to requests from remote clients, available for individuals' evalutation. Later, these evalutated individuals are inserted in the population when and if they are reported.

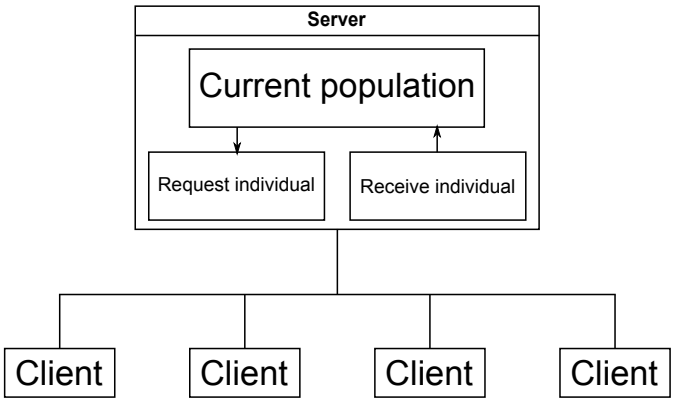

Figure 4.3: Client server schema for the Massively Distributed Genetic Algorithm

When starting the optimization process, the population is empty and requests from clients can be responded with fully randomized individuals or by individuals taken from an initial individuals table. Whether the population reaches a previ-

ously defined limit, crossover operations between individuals start happening for responding new requests from clients.

It is important to note that due to the fact that remote clients can experience random failures, because of their unknown conditions of operation, generating individuals by demand is the main aspect that ensure robustness to the process, since a non responding client will deliver no undesired state to the algorithm or the need for an individual to be recalculated by another client.

Another relevant aspect is that the heuristics for generating new individuals are randomized, allowing the asynchronous algorithm to generate as many unique individuals as are required to satisfy all potential client workers.

4.2.3 Generating new individuals (Genetic operators)

The main operation for generating a new individual is the crossover which is done by selecting two individuals (using an operation described in section 4.2.4) and applying the operation in equation 4.5 for each gene, i, from selected parents, thus generating the new individual.

$$G_i = R * Parent_{1_i} + (1 - R) * Parent_{2_i} \tag{4.5}$$

where R is a random generated number ranging from 0 to 1, which describes how close the newly generated individual will be to one of their parents.

In order to avoid premature convergence of the algorithm to a local optima, after the crossover operation, some individuals are chosen to be mutated, which can be an uniform or a side-shift mutation. When performing an uniform mutation, some genes are randomly replaced by new values, within the range that genes are allowed to receive. On the other hand, if a side-shift mutation is performed, some genes are chosen to shift towards a direction randomly chosen relative to their current position in order to allow some degree of fine search to happen near newly generated individuals.

Side-shift mutation applied in PCMDGA, resembles what was described as non-uniform mutation in [Michalewicz, 1996], but fitted to work with a continuously changing population. So a gene v is selected through a mutation rate, and then applying equation 4.6 to compute the new value.

$$v' = \begin{cases} v + \Delta(UB - v) & \text{if random value 0} \\ v - \Delta(v - LB) & \text{if random value 1} \end{cases} \tag{4.6}$$

where LB and UB are lower and upper bounds domain for variable v. The function $\Delta(y)$, described in equation 4.7, returns a value in the range $[0, y]$ that is proportional to a given strength r chosen randomly. In this way, we allow our search to spread in the space or being very locally depending on the strength variable.

$$\Delta(y) = y.(1 - r).s \tag{4.7}$$

In equation 4.7, y is the maximum value that the function can return and r is a random number from [0..1] that defines the mutation's strength. s is the strength of the mutation, which is a hard wired limit that defines the maximum shift that the gene can be pushed.

It is remarkable that newly generated individuals are not sent to evaluation if they are too close to others individuals in the population. Therefore, a metric of uniqueness is defined in section 4.2.5, to ensure a reasonable genetic variability in the algorithm's current population.

In this way, figure 4.4 describes the generation process of a new individual: two individuals are chosen by the process described in section 4.2.4, then a crossover is executed using equation 4.5. Finally, there is a probability of a mutation over this newly generated individual.

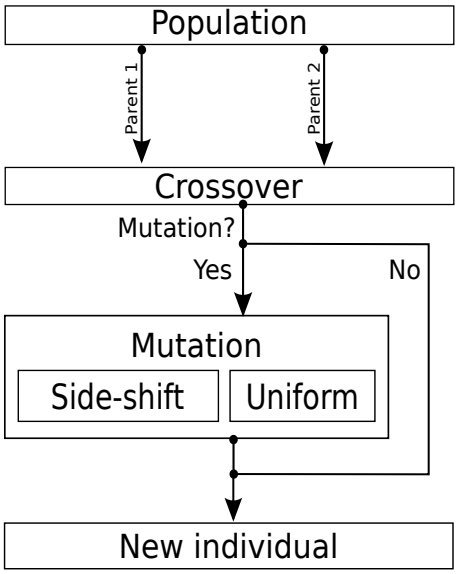

Figure 4.4: Flow for creating new individuals.

After all this creation process, provided that the individual is unique in the current population, it is sent for evaluation to any client available in the network. If a non-unique individual is generated, then the process is repeated until an unique individual comes out.

4.2.4 Selection

For selecting an individual, among n available, the probability curve, given by $f(x)$, must always follow the rule described in equation 4.8, so that all individuals, sorted in increasing order by their fitness, have a probability of being chosen, proportionally to their position in the fitness ranking.

$$\int_0^n f(x)dx = 1 \tag{4.8}$$

For example, in the case of a linear probability function, which was used in this work for selection, the probability of choosing the i^{th} individual among n is the dashed area shown in figure 4.5, and given by equation 4.9.

$$P_i = \int_{i-1}^{i} -\frac{2x}{n} + \frac{2}{n} dx \tag{4.9}$$

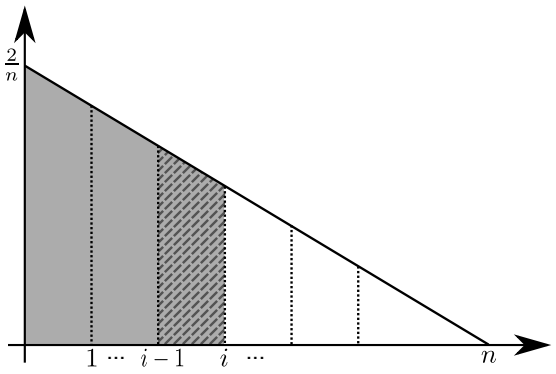

Figure 4.5: Probability distribution for choosing an individual

To easily implement a function for choosing an individual, an array of length n, can be created and each position filled with the accumulated probability of the latter individuals. This accumulated probability, in figure 4.5 for the i^{th} individual is the shaded area, which corresponds to the area between 0 and i. So for selecting an individual, it is only a matter of choosing a random number ranging from 0 to 1 and looking for the gap in the array where it belongs.

4.2.5 Individual uniqueness

An individual is considered unique when its euclidean distance from all the others individuals is greater than a threshold distance.

Checking whether two individuals are unique is important for continuous search, because the crossover method have high probability of creating individuals too close to others individuals in the search space, when no mutation is performed. Therefore, before any individual is sent to evaluation it is checked against all the current population: whether this individual is not unique, the process of creating a new individual is repeated, as commented in section 4.2.3.

Therefore, a metric of uniqueness of an individual was implemented, based in a fraction of the largest distance possible in the search space. Since the search

space is limited in all dimensions to the space between 0 and 1, an individual is unique if it has a distance greater than a given percentage from the $\sqrt{n}$, where n is the number of dimensions (as shown in figure 4.6), to all the others individuals placed in population.

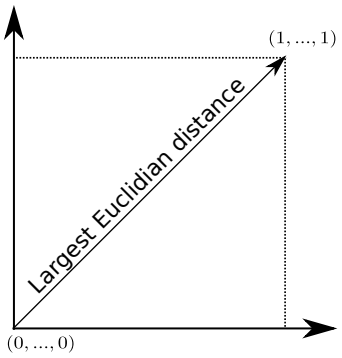

Figure 4.6: Largest distance possible in the search space

It is important to notice that, during the evolution, allowing the user to dynamically change the threshold which defines how distant individuals must be to be considered unique can help improve the local search when the algorithm is converging.

4.2.6 Receiving individuals

Whenever a client responds to the server with an evaluation of an individual, algorithm 1 will be executed.

Algorithm 1 Receive individual algorithm

```
1: if Population is not full then
2:     insert individual in the population
3: else
4:     replace an individual from the main table with the received individual
5: end if
```

In algorithm 1, the individual chosen to be replaced is select by a process similar to the one described in section 4.2.4, but with individuals sorted in in-

creasing order. This approach provides greater chances of lower fitness individuals being selected to be replaced.

To ensure elitism to the evolutionary process, a set of individuals with the highest fitness are never allowed to be chosen.

4.3 Optimizing Microcavities

4.3.1 Problem Description

As it has been described in section 2.2, the synthesis of semiconductor nanodevices, such as microcavities, is a challenging task because in order to create the desired device, the correct set of parameters must be chosen. The desired features are the highest possible Quality Factor (Q) and the correct position of cavity's resonance peak (λ_o).

Quality Factor ($Q = \Delta\lambda/\lambda_o$) is measured from the reflectance spectra, where the full width at half maximum (FWHM) of the resonance ($\Delta\lambda$) and the cavity resonance position (λ_o) are obtained directly.

It is well known that the resonance position is directly related to the thickness of the cavity layer. So, if a particular position of the resonance peak is desirable, the thickness of the cavity layer is easily defined by $L_c = m(\lambda_o/2n_c)$, for an integer number m and a cavity with refractive index n_c. Moreover, the thickness of the layers in the DBR mirror is given by $L_{DBR} = \lambda_o/4n_i$, where n_i is the refractive index of each layer. However, the remaining parameters may shift slightly the peak position. So, they have to be optimized in order to minimize as much as possible this shift. Figure 4.7 shows how a growth error affected the position of the resonance peak for 1900nm.

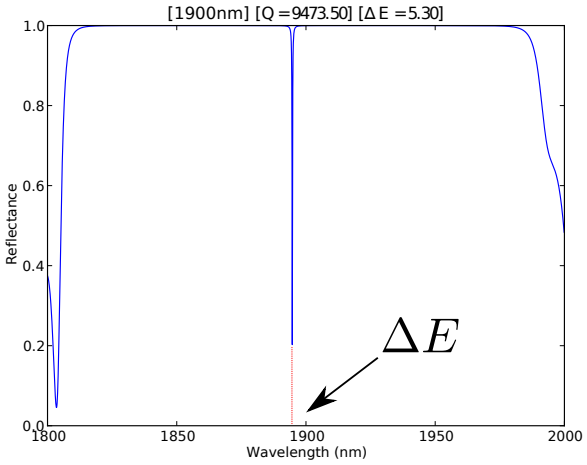

Figure 4.7: Resonance peak shift.

The problem of microcavities growth is to look for the best set of parameters before the experimental synthesis of the desired nanodevice. Such parameters will guide the experimental physicist in the slow and expensive process of growth. Whereas the relationship between the desired position of the resonance peak and the thickness of the layers are well known, the algorithm has to search for the others parameters involved in the growth process. In this way, the parameters involved in the microcavities optimization problem (MO), as shown in figure 4.8, are:

- Number of layers in the inferior DBR mirror (NL1);
- Number of layers in the superior DBR mirror (NL2);
- Aluminium concentration in the first layer of the pair (CP1);
- Aluminium concentration in the second layer of the pair (CP2);
- Aluminium concentration in the layer of the cavity (CC).

Where CC, CP1 and CP2 are percentual concentration values, ranging from 0 to 1, and NL1 and NL2 are integer numbers between 0 and 30, whose limits were defined to comply with demands from experts.

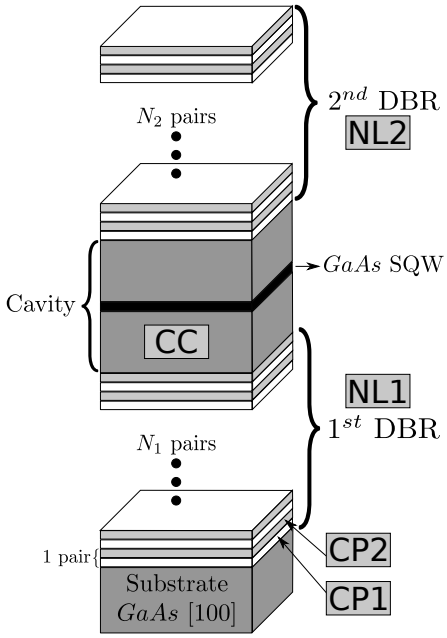

Figure 4.8: Parameters for optimization.

So, given a microcavity with its desirable resonance peak and a set of parameters to be established, the MO problem consists in chosing the set of parameters, such that the Q is maximized and ΔE is minimized.

In this way, for each structure it has been measured the Quality Factor (Q) and the error deviation (ΔE) to the desired position of the resonance peak. These variables are related according to the equation 4.10.

$$F = Q\left(1 - \left(\frac{\Delta E}{\Delta E + n}\right)\right) \tag{4.10}$$

So the MO problem can be defined as:

$$Solution = MAX(F) \tag{4.11}$$

where Q and ΔE in F is given by $f(NL1, NL2, CP1, CP2, CC)$, where f is the simulation presented in [Coelho et al., 2013].

Equation 4.10 was chosen due to the fact that ΔE has no known limit. Let $f(\Delta E) = \left(\frac{\Delta E}{\Delta E+n}\right)$, then $\lim_{\Delta E \to +\infty} f(\Delta E) = 1$, thus this part of the equation works as a weight, ranging from 0% to 100% on how the error impacts in the fitness final

value. If the error is zero, the impact is null, otherwise, if the error is to high, the impact will be approaching 100% of the quality. Figure 4.9 shows how changing n impacts on the value of $f(\Delta E)$.

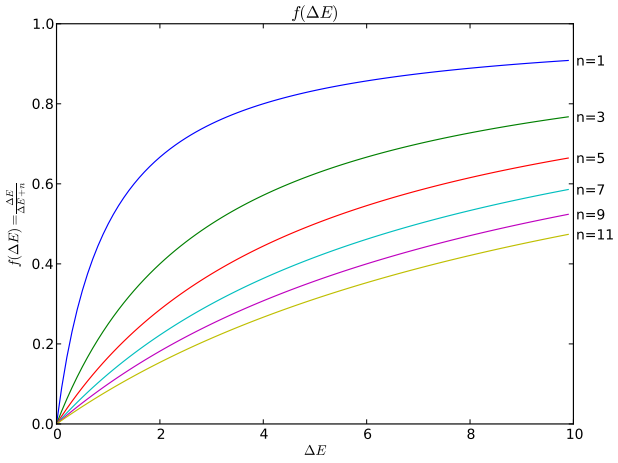

Figure 4.9: Impact of varying n on Q

It has been verified that ΔE is strongly related to the growth inaccuracies and the optimized parameters haven't a great influence in the error, but can slightly minimize it. So, the main feature to be optimized is the Q value, but still considering the ΔE.

The major inaccuracy during the synthesis process is related to the thickness of the layers and their roughness. The roughness problem can be minimized with the use of Molecular Beam Epitaxy (MBE) technique in the growth process. Since our target devices are in nanometer scale, small variations in layers thickness can impact significantly the final result. Thus, the optimization process developed in this work has to deal with uncertainty. According to experts, during the growth process two different problems can occur: (a) the MBE used to grow the device is calibrated to a specific deposition rate. This deposition rate defines how many atomic layers are deposited per second. An error of about 1% can occur in this process, leading to a thickness variation in all layers of the device; (b) during the deposition of each layer a local error, also equal to 1%, can happen, causing the device to have layers with different thicknesses.

Nevertheless, although the process of synthesis of nanoscale semiconductors is well developed, there is still some inaccuracies not controlled by experts. Therefore, in this work is intended to search for a set of parameters that could lead to the development of good devices even if inaccuracies occur during the growth process.

In order to deal with this uncertainty, each set of parameters representing a solution has its fitness evaluated against 10 different microcavities structures, in which the first structure presents layers thickness in the DBR mirror given by $L_{DBR} = \lambda_o/4n_i$, where n_i is the refractive index of each layer, as described earlier. The next nine structures are randomly generated considering the 1% error in calibration phase and the 1% error in the growth of each layer. It has been decided to use ten structures because of the time consuming simulation of each individual and due to preliminary testing with a larger number of structures showing small changes in results.

So, to ensure that the experimental physist will be able to grow a microcavity with the desired features, the MO problem is now defined as:

$$Solution_{min} = MAX\left(MIN(F_i)\right); (i = 1, 2, ..., 10) \tag{4.12}$$

where F_i is the evaluation of the i^{th} struture.

Also, the average MO problem is defined and used to compare with the previous solution. In this case:

$$Solution_{average} = MAX\left(\sum_{i=1}^{10} \frac{F_i}{10}\right); (i = 1, 2, ..., 10) \tag{4.13}$$

Finally, an optimization problem that does not consider the robustness can be defined as:

$$Solution_{max} = MAX\left(MAX\left(F_i\right)\right); (i = 1, 2, ..., 10) \tag{4.14}$$

The result of this optimization problem can deliver the highest possible evalutation, but it does not ensure that the grown microcavity will present the desired features due to uncertainty.

4.3.2 Applied optimization algorithm

The Genetic Algorithm implemented for optimizing these microcavities while building the initial population, randomly tries to generate individuals without null fitness until it fills the initial population or it reaches a defined limit of tries. After the initial population is built, the algorithm works as described in section 4.1, with individuals whose chromosomes are built according to the parameters described in section 4.3.1.

Each gene in the chromosome holds a floating point value ranging from 0 to 1. The first three genes are the Aluminium concentration, x, of the two layers in the pair of the DBR mirrors and in the cavity layer, according to figure 2.3. The last two genes represent the number of pairs of layers on each DBR mirror. In order to not encumber the future physical synthesis of the device, the number of pairs of layers was limited to 30 in each mirror. These individuals are evaluated through the simulation described in [Coelho et al., 2013] and the strategies described in section 4.3.1.

Chapter 5

Experimental results

5.1 Photonic Crystal cavity design

For designing photonic cavities with high Quality Factor, PCMDGA, described in section 4.2.2, has been applied in conjunction with MEEP [Oskooi et al., 2010] for FDTD simulations in clients spread across multiple locations. These clients includes personal computers, powerful computing servers in UFMG's laboratories and multi-processor clusters from LNCC and UFMG. Because of the long time required by the optimization process during the experiments, these clients were randomly attached and detached from the process, due to a multitude of factors such as power shortages and maintenance routines.

This scenario displays the heterogeneous nature of the implemented algorithm and makes clear that every experiment is unique. As commented in [Desell et al., 2010], the order in which requests for new individuals are done and their respective responses with simulation's results greatly impacts the overall evolutionary process. Thus, in real world scenarios, it is a hard task to reproduce the conditions in which each experiment was developed.

Our goal is to reach similar or better crystals than what has been achieved in [Saucer and Sih, 2013]. For doing so, a MEEP script, for physics simulation, was developed with geometric parameters described in section 4.2 and the slab's properties in table 5.1.

Resolution	20
Edge shift	0.15
Decay time	500
Number of padding holes	8
Hole radius	0.29
Slab thickness	0.6
PML	1
Pulse's frequency center	0.273712876505613
Pulse's width	0.01

Table 5.1: Photonic Crystal experiments parameters

MEEP discretizes every structure in space and time, and that is specified by the *resolution* variable, which gives the number of pixels per distance unit. Before the holes' patterns in the slab, there is an *Edge shift*, which, effectively, is the distance before the border of the first hole in every slab's corner. For defining the simulation time, there is a *Decay time*, in MEEP's units. Before the cavity, there are a *number of padding holes* which, actually, are the number of holes, before the missing holes in the middle of the slab. The *Perfectly Matched Layer (PML)* is the absorbing boundary condition in FDTD, described in [Berenger, 1994], which is the surrounding computational cell with a medium that in theory absorbs without any reflection electromagnetic waves at all frequencies and angles of incidence. For analyzing the behaviour of the light within the slabs, a gaussian pulse of light with a defined frequency center and width is used in the slab's center.

These parameters were defined in talks with physists Juan Pablo Vasco (UFMG) and Timothy Saucer (University of Michigan) which were working with these photonic crystals cavities.

After setting up the simulation's conditions, in order to optimize the design of the photonic crystal, the parameters in table 5.2 were used to set up the PCMDGA.

Elitist set length	5
Global mutation rate	10%
Maximum individuals in population	100
Mutation strength	50%
Side-shift mutation strength	30%
Number of decimal digits	5
Uniform mutation rate	50%
Uniqueness threshold	1%

Table 5.2: PCMDGA parameters

The elistist set length represents the size of the set of the best individuals in the current population which can never be selected to be replaced. This procedure ensures an elitist behavior, thus, preserving the evolution of the population.

In this way, as described in section 4.2, to make sure that the algorithm does a broad search, 10% of all generated individuals are select to perform some kind of mutation, in which 50% will be a Side-shift mutation and the other 50% mutated by an uniform mutation. When performing a Side-shift mutation, there is a strength threshold which limits in 30% how far the gene can be shifted, relative to the current position of the gene and the upper or lower limit.

Therefore, to enable a broad search, each new generated individual, must be at least 1% of the maximum distance in the search space (which in this case is $\sqrt{12}$) far from all the other individuals in the current population. In latter stages of the evolution, this distance can be reduced by the user in order to allow a more narrow search around the best individuals, thus enabling a local optimization.

By applying these parameters in PCMDGA, during the course of four months it was possible to run three experiments whose details are displayed in table 5.3.

Experiment	**1**	**2**	**3**
Pulse frequency	0.2737	0.2737	0.26
Duration	35 days	38 days	43 days
Evaluations' amount	8430	4565	7000
Best Q found	338173.46970151	336267.3187271	334516.66857112
Best Q insertion number	7931	3241	5336
Average simulation time (s)	13577.16	7251.19	21369.36
Estimated clients' amount	50	30	60

Table 5.3: Photonic Crystal experiments results

The amount of evaluations in each experiment is fairly different from each other because of the availability of resources during the experiment's course. In the first experiment, there were around 15 extremely fast machines (evaluating individuals within 3500 seconds), working along 35 very slow machines (taking 50,000 seconds for each individual), what explains the higher amount of evaluations and average of simulation time. In a different scenario, the second experiment was running, mainly, with fast machines, which explains the reduced average time of each simulation and the fewer individuals evaluated before the best were found. In the third experiment, LNCC's cluster were introduced in which individuals were evaluated within a fair amount of time (around 13,000 seconds) along those slow machines from the first experiment. The *Best Q insertion number* gives the time in which the simulation's best individual has been inserted in the population. In this way, it is possible to see that when only faster machines were employed, the results arrived earlier, which is the case of the second experiment.

These analysis aren't conclusive, because there were not enough time to perform extensive experiments in each scenario, due to the computational complexity around the FDTD's simulation.

Due to complexity of PCMDGA, it is almost impossible to precisely know the amount of clients that were actually generating results for the algorithm over the course of time. The estimation is based on the number of MEEP's process started in the clusters and machines available in the beginning of each experiment.

Since there is no generation concept, a way to track the algorithm's evolution

is by plotting the increase in best fitness in current population in each individual insertion. Figures 5.1 and 5.2 show how the quality factor for each experiment performed for pulse's frequency of 0.27371 and 0.26 respectively. Each rung transition in the chart represents that an individual better than all the others in current population has been inserted.

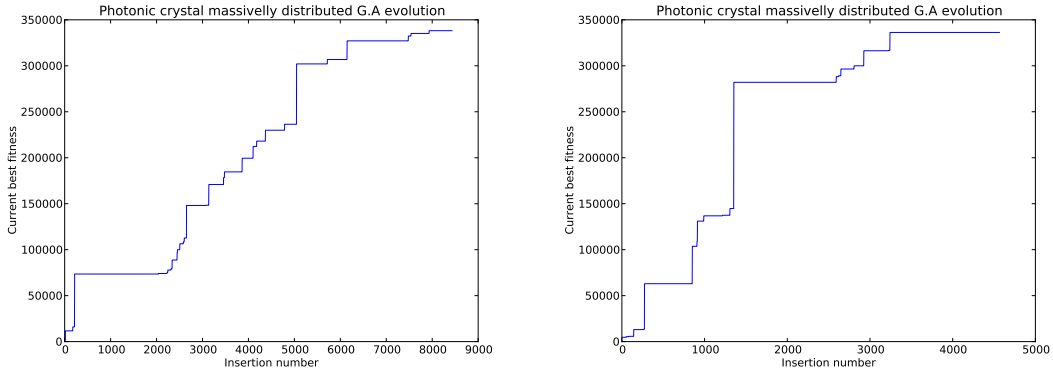

(a) (b)

Figure 5.1: Photonic crystal PCMDGA evolution with frequency center at 0.27371. (a) Experiment 1 and (b) Experiment 2.

In figure 5.2, all the parameters advertised in table 5.2 has been kept the same, with the exception of the frequency center, which was changed to 0.26, in order to see whether this parameter would deliver a different Quality Factor in the evolution process.

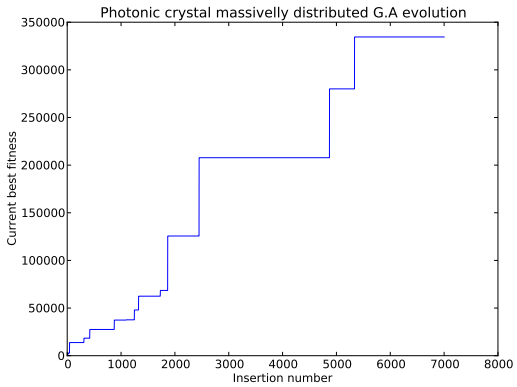

Figure 5.2: Photonic crystal PCMDGA evolution with frequency center at 0.26 for Experiment 3.

The evolutionary process was arbitrarily halted when the evolution seems to not be receiving any new improvements. Figure 5.3 displays how the best crystal found in each experiment looks like. These crystals holds similarities with that found in [Saucer and Sih, 2013] and are a clue about the behaviour of *L3* cavity towards it's optimum.

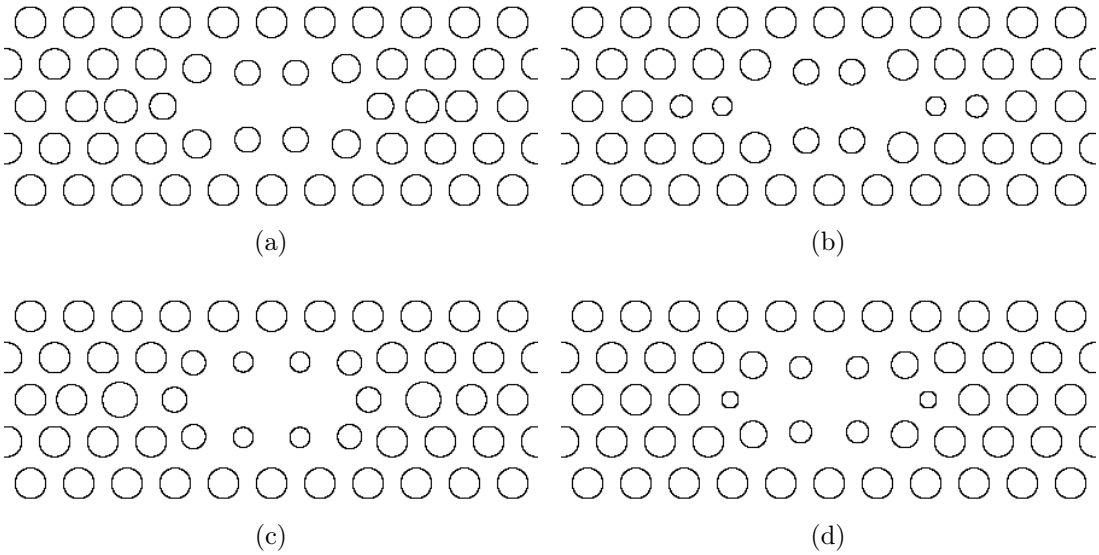

Figure 5.3: (a), (b) and (c) are the best crystals found in experiments 1, 2 and 3, respectively. (d) is the best from [Saucer and Sih, 2013].

In attempts to reproduce results from [Saucer and Sih, 2013], which has advertised a Quality Factor of 560,000, the best Q that could be achieved through the experiments with the code provided by the author were 148,749.57, with mode volume of 0.858 when the frequency were set to 0.27371 and 12 padding holes with resolution of 40. By comparison, in the same conditions, the best crystal found in this work has a Quality Factor of 613,158.15 and mode volume of 0.7683.

Table 5.4 compares the best results from each experiment performed in this work, with that performed by [Saucer and Sih, 2013]. To check accuracy of the crystal, [Saucer and Sih, 2013] recomended increasing the number of padding holes to 12 and the resolution to 40. In this way, it is easy to see that the results from this work were accurate and had performed better than that from [Saucer and Sih, 2013].

	Results for resolution of 20		Results for resolution of 40	
	Quality	Mode volume	Quality	Mode volume
Experiment 1	338173.47	1.089	550540.27	0.900
Experiment 2	336267.32	1.048	613158.15	0.768
Experiment 3	334516.66	0.895	106623.98	0.951
[Saucer and Sih, 2013]	101180.87	0.869	148749.57	0.858

Table 5.4: Best crystals results comparison.

It is important to note that the optimization process could not be held in the resolution of 40, due to the increase in the evalution time, which would be unfeasible.

The importance of reducing the mode volume of cavities were an unknown fact during the early stages of this work, so there were no available time to conduct optimizations for this target, thus, all the optimizations performed by PCMDGA only accounted leveraging the Quality Factor. However, in this work the mode volume has been improved.

As discussed in section 4.2, the simulation has been done using genes that range from 0.0 to 1.0 and each value were latter interpolated to match the actual parameters for the simulator. This scenario, added to the fact that there were 5 decimals in each of the 12 genes, deliver a search space of 10^{60} possible individuals, which in turn would be calculated by the FDTD simulator. By analysing table 5.3 it is possible to see that with less than 7000 evaluations a good result were achieved,

which is much less than those 15000 simulations required by the algorithm applied in [Saucer and Sih, 2013]. These results show that only a small portion of the search space needs to be explored in order to reach results better than the best currently found in literature.

In table 5.5 there is a comparison of the attributes of each hole in the cavity, relative to the origin and placed in the third quadrant which are latter, mirrored to all the other quandrants. These attributes are from the bests crystals found in this work and in [Saucer and Sih, 2013] and displayed in figure 5.3.

Hole ID	Attribute	Experiment 1	Experiment 2	Experiment 3	From Saucer and Sih [2013]
0	x	-2.25201	-2.20744	-2.0162	***-2.05***
	radius	0.249333	0.171196	0.228862	***0.15***
1	x	-3.12258	-3.0538	-3.14725	-3.00
	radius	0.309233	0.20052	0.332879	0.29
2	x	-3.93787	-3.97532	-4.14718	-4.00
	radius	0.298311	0.290177	0.284104	0.29
3	x	-0.4988	0.473688	-0.588032	***-0.59***
	y	-0.687753	0.707881	-0.779081	***-0.67***
	radius	0.233027	0.233676	0.17964	***0.20***
4	x	-1.54918	-1.52973	-1.61842	***-1.57***
	y	-0.778585	-0.853225	-0.764145	***-0.72***
	radius	0.263787	0.284348	0.222236	***0.25***

Table 5.5: Best crystals features comparison, relative to the origin. The Holes IDs are according to figure 4.1.

It is important to note that in [Saucer and Sih, 2013] it were optimized 8 parameters, which are the values in bold face in table 5.5.

5.2 Microcavities experiments

For each microcavity structure with different resonance peak ranging from 700nm to 2000nm (increasing by 100nm in each experiment) it has been optimized five parameters: the number of layers in the top and bottom of DBR mirrors and the aluminium's concentration in three distinct layers (each layer of the pair that constitute the DBR mirror and the cavity).

The Genetic Algorithm applied in this optimization (described in section 4.3.2) has been set up, for all experiments, with parameters from table 5.6.

Number of individuals per generation	40
Number of generations	200
Elitist set length	5
Mutation rate	10%
Uniform mutation rate	50%
Non-uniform mutation rate	50%

Table 5.6: MCGA parameters

The mutation rates described above means that 10% of the newly generated individuals are chosen to be mutated and among those, 50% are going to be uniformly mutated and the other 50% will be non-uniformly mutated.

For each resonance peak it has been performed optimizations considering the three fitness strategies described in section 4.3. It is important to remember that the optimization goal is to look for structures that could present high Quality Factor (Q) and the smaller possible shift in the position of the resonance peak. Figures 5.4, 5.5 and 5.6 are results of the fitness curves, for resonance peaks of 800nm, 1400nm and 2000nm. In these curves, it is shown how each strategy evolved in an average of the best individuals from each generation in 15 runs of the algorithm. Evolution curves for all the other experiments can be found in appendix B.1.

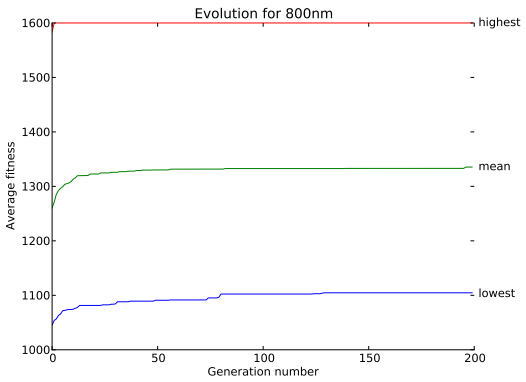

Figure 5.4: Evolution for 800nm

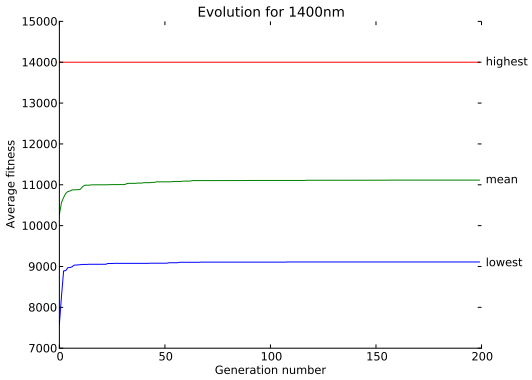

Figure 5.5: Evolution for 1400nm

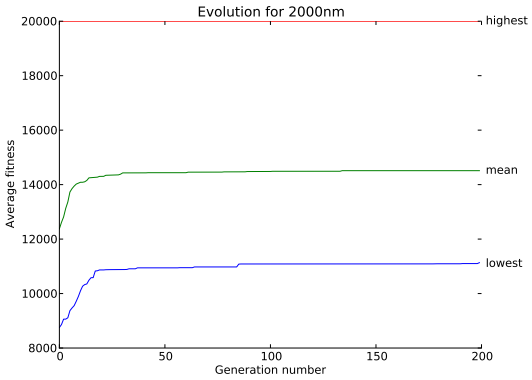

Figure 5.6: Evolution for 2000nm

The results of the best structure found in each experiment are shown in table 5.8. This table shows error deviation, ΔE, Quality Factor, Q, and evaluation value for each of ten structures of the best individual found in each resonance peak for each strategy.

In these experiments, it is expected that the first structure, labeled as 1, presents the best evaluations (highest Q and lowest ΔE), due to the fact that this structure is built without errors during the growth. So all the others structures represents those with some error during the growth, therefore, showing how inaccuracies can impact the quality factor. However, in some cases a structure other

than the first one, had shown a better quality, probably because that growth issue has delivered a good structure for that resonance peak.

As expected, in the evolution charts, as shown in figures 5.4, 5.5 and 5.6, the highest fitness evaluation strategy presents the best fitness value, as it takes the maximum evaluation value considering the ten different microcavities structures. The experiments considering only the best evaluation has the advantage that at least one structure will deliver a great quality, thus reaching the desired function in the given resonance peak. However, the set of parameters delivered by the evolutionary process, in this strategy, will not ensure that when some error in the growth happens, the grown struture will behave as expected. Therefore, this strategy doesn't ensure robustness, as can be seen in results from table 5.8. This fact is best seen through the high standard deviation value for highest evaluation strategy which means that there is a huge variation in the quality from the worst to the best microcavity.

On the other hand, the lowest evaluation strategy, as it takes the worst evaluation value from the ten structures, evolves to a lower fitness value. This strategy ensures that, in the worst case, when a microcavity with some error is grown, a good Quality Factor device is going to be delivered. Actually, this strategy has the warranty of robustness in the parameter set delivered by the evolutionary process, due to the fact that worst device has some quality ensured. Generally, the lowest evaluation strategy tends to present the most robust result. However, when analysing the data from experiments, shown in table 5.8, it is possible to see that the evolution considering the average of the ten strutures, also delivers a robust parameter set for all resonance peaks. In some cases, the average strategy outperform the robusteness presented by the lowest evaluation strategy, such as in the case of resonance peak of 1600nm, where the worst case presented by the average strategy is better than that presented by the lowest evaluation strategy.

In results from table 5.8, results with is a high average and a low standard deviation in the fitness' values, it means that growth problems will not deeply impact on the overall quality of the final device, due to the fact that there is reduced variance in the quality delivered by the parameter set.

Table 5.7 shows all the parameters set for each resonance peak and strategy studied in this work, which are needed to build structures presented in table 5.8. These structures will look like that from figure 2.3.

Frequency	Fitness strategy	*Al* concentration in first layer	*Al* concentration in second layer	Cavity's *Al* concentration	Layer's pairs in Inferior mirror	Layer's pairs in Superior mirror
700	lowest	0.41	0.91	0.97	27	30
700	mean	0.54	0.98	0.74	29	30
700	highest	0.51	0.94	0.65	29	30
800	lowest	0.33	0.89	0.58	26	30
800	mean	0.35	0.98	0.55	26	30
800	highest	0.28	0.90	0.57	27	28
900	lowest	0.95	0.07	0.72	27	26
900	mean	0.96	0.02	0.78	25	27
900	highest	0.14	0.85	0.59	24	26
1000	lowest	0.97	0.07	0.80	27	28
1000	mean	0.97	0.07	0.71	26	27
1000	highest	0.14	0.91	0.46	23	25
1100	lowest	0.98	0.05	0.85	27	28
1100	mean	0.97	0.10	0.80	27	26
1100	highest	0.94	0.05	0.46	25	26
1200	lowest	0.99	0.06	0.94	25	26
1200	mean	0.99	0.01	0.84	25	27
1200	highest	0.94	0.09	0.71	27	26
1300	lowest	1.00	0.03	0.89	27	25
1300	mean	0.98	0.06	0.89	26	27
1300	highest	0.99	0.11	0.48	25	26
1400	lowest	0.07	0.98	0.95	23	24
1400	mean	0.97	0.06	0.97	29	26
1400	highest	0.94	0.09	0.57	27	27
1500	lowest	0.99	0.01	0.86	30	24
1500	mean	0.99	0.01	0.86	30	24
1500	highest	0.93	0.05	0.12	27	29
1600	lowest	0.09	1.00	0.92	23	26
1600	mean	0.99	0.03	0.99	29	28
1600	highest	0.92	0.05	0.61	28	28
1700	lowest	0.06	0.98	0.55	23	28
1700	mean	0.08	0.99	0.41	19	28
1700	highest	0.97	0.04	0.85	30	25
1800	lowest	0.99	0.07	0.89	27	27
1800	mean	0.10	0.99	0.90	25	30
1800	highest	0.98	0.07	0.90	30	26
1900	lowest	0.07	0.97	0.62	23	28
1900	mean	0.98	0.07	0.91	30	26
1900	highest	0.88	0.08	0.13	30	30
2000	lowest	0.08	1.00	0.64	22	29
2000	mean	0.08	0.99	0.71	25	27
2000	highest	0.10	0.89	0.59	26	28

Table 5.7: Best parameters found for microcavities

When analysing how the Quality Factor evolves as a function of the resonance peak, it is remarkable that the best Quality Factor found, after $900nm$, increases linearly as the resonance peak increase, as can be seen in figure 5.7. In the experiments performed for resonance peaks lower than $700nm$, there were no Quality Factor found by the evolutionary process.

Figure 5.7: Best quality factor found as a function of the resonance peak.

Figures 5.8, 5.9 and 5.10 displays the reflectance spectrum for the best structures found in this work for resonance peak of 800nm, 1400nm and 2000nm. All the other structures' resonance peaks are shown appendix B.2. These structures are the best shown in table 5.8 among the ten microcavities applied in the optimization process. The parameters needed to build these structures are shown in table 5.7.

As can be observed in these reflectance spectra, all resonance peaks are tightly aligned in their respective frequency peaks, as set before the optimization tooks place. This behavior of being very thin at a given resonance peak caracterizes a good Quality Factor, and demonstrates that the optimization has, successfully, found the parameters needed to match each resonance peak.

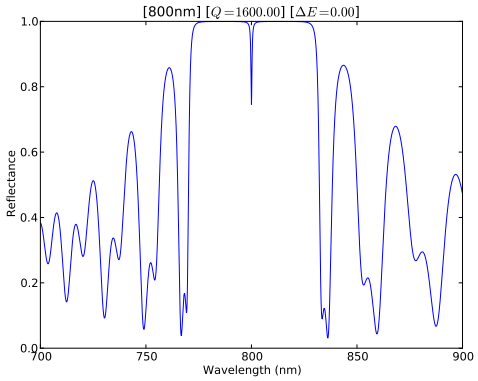

Figure 5.8: Reflectance for 800nm

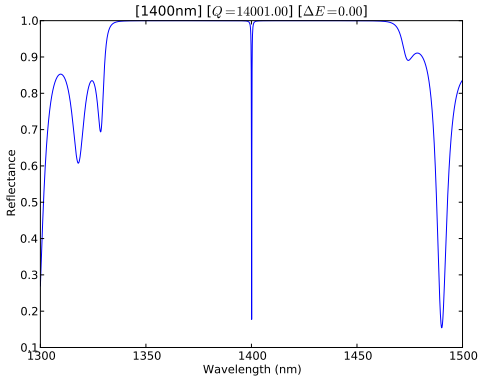

Figure 5.9: Reflectance for 1400nm

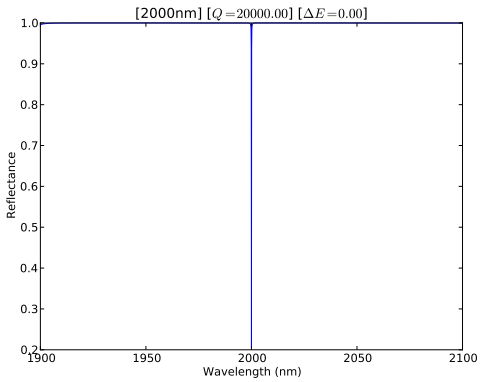

Figure 5.10: Reflectance for 2000nm

In order to demonstrate how hard is to, randomly, find an individual in the search space with a fitness greater than zero, figure 5.11 plots the number of randomly generated individuals that the algorithm has tried for constructing the initial population. Inside each box, there is the average number of individuals that were effectivelly found until the initial population was filled or the 20,000 limit of tries has been exhausted in the 15 experiments executed. It is remarkable that when the lowest evaluated structure is being used as fitness, it is harder to find individuals with fitness greater than zero. As discussed in section 4.3.2 randomly trying to find individuals which holds some Quality Factor, is a measure that ensures that the evolution has a high probability of going through some optimization, rather than randomly crossing over individuals that will never reach any quality.

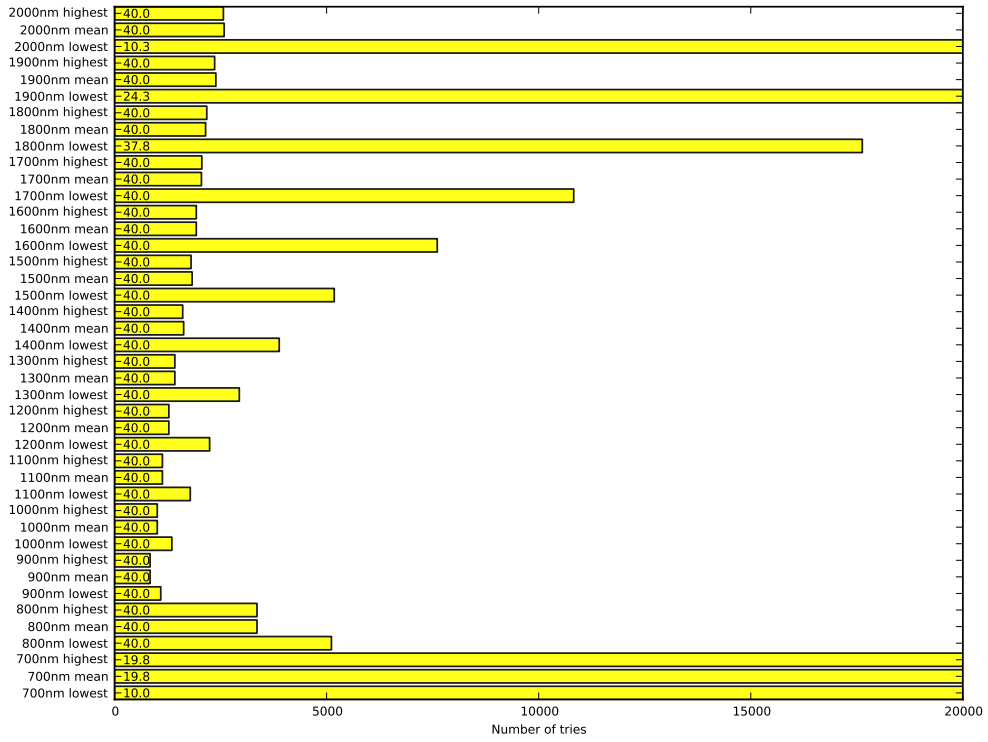

Figure 5.11: Average of the number of tries the algorithm has randomly made to find an individual with a fitness value greater than zero, in the 15 experiments executed. Inside each box is the average number of individuals found.

Table 5.8: Structures Fitness for each resonance peak.

	700nm									800nm								
	Fitness: Highest Evaluation			Fitness: Average Evaluation			Fitness: Lowest Evaluation			Fitness: Highest Evaluation			Fitness: Average Evaluation			Fitness: Lowest Evaluation		
Structure	ΔE	Q	F_i	ΔE	Q	F_i	ΔE	Q	F_i	ΔE	Q	F_i	ΔE	Q	F_i	ΔE	Q	F_i
1	0.00	700.00	700.00	0.00	700.00	700.00	0.00	636.36	636.36	0.00	1600.00	1600.00	0.00	1600.00	1600.00	0.00	1600.00	1600.00
2	2.20	697.80	571.97	2.20	697.80	571.97	2.00	698.00	581.67	2.40	1329.33	1072.04	2.40	1329.33	1072.04	2.50	1595.00	1276.00
3	2.10	697.90	576.78	2.00	698.00	581.67	1.80	698.20	591.70	2.20	1329.67	1089.89	1.90	1596.20	1341.34	2.00	1596.00	1330.00
4	1.00	0.00	0.00	1.00	699.00	635.46	0.50	699.50	666.19	0.60	1332.33	1256.92	0.60	1598.80	1508.30	0.60	1598.80	1508.30
5	2.20	697.80	571.97	2.20	697.80	571.97	2.40	697.60	562.58	3.00	1328.33	1021.79	2.70	1594.60	1255.59	2.70	1594.60	1255.59
6	3.00	697.00	536.15	3.00	697.00	536.15	2.60	697.40	553.49	3.10	1328.17	1013.87	3.60	1592.80	1171.18	3.60	1592.80	1171.18
7	2.00	698.00	581.67	1.90	698.10	586.64	2.10	697.90	576.78	2.40	1329.33	1072.04	2.10	1595.80	1318.84	2.20	1595.60	1307.87
8	0.80	699.20	647.41	0.80	699.20	647.41	1.00	699.00	635.46	1.30	1597.40	1413.63	0.90	1598.20	1466.24	0.90	1598.20	1466.24
9	1.00	699.00	635.46	1.00	699.00	635.46	1.10	635.36	572.40	1.30	1331.17	1178.02	1.40	1597.20	1401.05	1.40	1331.00	1167.54
10	0.40	699.60	672.69	0.40	699.60	672.69	0.80	699.20	647.41	0.90	1331.83	1221.87	1.00	1598.00	1452.73	1.00	1598.00	1452.73
mean	1.47	628.63	549.41	1.45	**698.55**	**613.94**	**1.43**	685.85	602.40	1.72	1383.76	1194.01	**1.66**	**1570.09**	**1358.73**	1.69	1570.00	1353.55
stdev	0.96	220.88	199.92	0.95	**0.95**	51.92	**0.87**	26.36	**40.03**	1.05	113.30	188.78	1.09	84.62	160.78	1.10	**84.00**	**146.56**

	900nm									1000nm								
	Fitness: Highest Evaluation			Fitness: Average Evaluation			Fitness: Lowest Evaluation			Fitness: Highest Evaluation			Fitness: Average Evaluation			Fitness: Lowest Evaluation		
Structure	ΔE	Q	F_i	ΔE	Q	F_i	ΔE	Q	F_i	ΔE	Q	F_i	ΔE	Q	F_i	ΔE	Q	F_i
1	0.00	9000.00	9000.00	2.00	9020.00	7516.67	1.80	9018.00	7642.37	0.00	10000.00	10000.00	1.80	10018.00	8489.83	2.00	10020.00	8350.00
2	2.60	8974.00	7122.22	0.70	8993.00	8404.67	0.90	8991.00	8248.62	2.50	9975.00	7980.00	1.30	9987.00	8838.05	1.00	9990.00	9081.82
3	2.60	8974.00	7122.22	0.00	8999.00	8999.00	0.60	8994.00	8484.91	3.30	9967.00	7493.98	0.50	9995.00	9519.05	0.70	9993.00	9339.25
4	0.60	4497.00	4242.45	1.40	9014.00	7907.02	1.20	9012.00	8046.43	1.10	9989.00	8999.10	1.10	10011.00	9018.92	1.30	10013.00	8861.06
5	3.00	8970.00	6900.00	0.70	8993.00	8404.67	1.70	8983.00	7677.78	3.60	4982.00	3663.24	1.80	9982.00	8459.32	2.00	9980.00	8316.67
6	3.50	8965.00	6640.74	1.30	8987.00	7953.10	1.60	8984.00	7744.83	3.60	9964.00	7326.47	2.90	9971.00	7729.46	1.90	9981.00	8387.39
7	2.90	8971.00	6954.26	0.30	8997.00	8734.95	0.90	8991.00	8248.62	3.60	4982.00	3663.24	0.70	9993.00	9339.25	1.00	9990.00	9081.82
8	1.20	4494.00	4012.50	1.30	9013.00	7976.11	0.20	9002.00	8825.49	1.00	4995.00	4540.91	0.60	10006.00	9439.62	0.20	10002.00	9805.88
9	2.00	8980.00	7483.33	0.30	9003.00	8740.78	0.40	9004.00	8657.69	2.00	9980.00	8316.67	0.00	10000.00	10000.00	0.40	10004.00	9619.23
10	0.80	8992.00	8325.93	1.00	9010.00	8190.91	0.70	9007.00	8417.76	0.90	4995.50	4583.03	0.40	10004.00	9619.23	0.80	10008.00	9266.67
mean	1.92	8081.70	6780.36	**0.90**	**9002.90**	**8282.79**	1.00	8998.60	8199.45	2.16	7982.95	6656.66	**1.11**	9996.70	**9045.27**	1.13	**9998.10**	9010.98
stdev	1.19	1890.12	1570.90	0.61	**10.89**	459.01	**0.56**	11.83	**414.79**	1.35	2577.13	2333.79	0.86	14.13	677.76	**0.65**	**13.44**	**528.66**

	1100nm									1200nm								
	Fitness: Highest Evaluation			Fitness: Average Evaluation			Fitness: Lowest Evaluation			Fitness: Highest Evaluation			Fitness: Average Evaluation			Fitness: Lowest Evaluation		
Structure	ΔE	Q	F_i	ΔE	Q	F_i	ΔE	Q	F_i	ΔE	Q	F_i	ΔE	Q	F_i	ΔE	Q	F_i
1	1.00	5505.00	5004.55	1.90	11019.00	9259.66	2.10	11021.00	9108.26	1.60	6008.00	5179.31	2.10	12021.00	9934.71	2.30	12023.00	9774.80
2	2.40	10976.00	8851.61	1.50	10985.00	9552.17	1.30	10987.00	9723.01	2.20	11978.00	9818.03	1.70	11983.00	10241.90	1.50	11985.00	10421.70
3	1.70	10983.00	9387.18	1.20	10988.00	9810.71	1.00	10990.00	9990.91	1.80	11982.00	10154.20	0.90	11991.00	11000.90	0.70	11993.00	11208.40
4	0.20	11002.00	10786.30	1.10	11011.00	9919.82	1.30	11013.00	9746.02	0.70	12007.00	11221.50	1.20	12012.00	10725.00	1.40	12014.00	10538.60
5	2.50	5487.50	4390.00	2.60	10974.00	8709.52	2.40	10976.00	8851.61	3.30	11967.00	8997.74	1.80	11982.00	10154.20	1.60	11984.00	10331.00
6	3.20	5484.00	4154.55	2.50	10975.00	8780.00	2.30	10977.00	8924.39	3.30	11967.00	8997.74	2.60	11974.00	9503.17	2.40	11976.00	9658.06
7	1.90	5490.50	4613.87	1.50	10985.00	9552.17	1.30	10987.00	9723.01	2.20	11978.00	9818.03	1.10	11989.00	10800.90	0.90	11991.00	11000.90
8	0.00	11001.00	11001.00	0.10	10999.00	10890.10	0.00	11000.00	11000.00	0.60	11994.00	11315.10	1.10	12011.00	10820.70	1.30	12013.00	10631.00
9	1.10	5494.50	4950.00	0.00	11001.00	11001.00	0.30	11003.00	10682.50	0.40	5998.00	5767.31	0.30	11997.00	11647.60	0.10	11999.00	11880.20
10	0.30	5498.50	5338.35	0.50	11005.00	10481.00	0.70	11007.00	10286.90	0.00	12001.00	12001.00	0.60	12006.00	11326.40	0.80	12008.00	11118.50
mean	1.43	7692.20	6847.74	1.29	10994.20	9795.62	**1.27**	**10996.10**	**9803.66**	1.61	10788.00	9327.00	1.34	11996.60	10615.55	**1.30**	**11998.60**	**10656.32**
stdev	1.09	2838.74	2804.50	0.91	15.16	799.52	**0.82**	**15.13**	**718.92**	1.17	2521.95	2259.55	**0.70**	**15.37**	**654.96**	0.71	**15.37**	673.63

Table 5.8: Structures Fitness for each resonance peak.

	1300nm									1400nm								
	Fitness: Highest Evaluation			Fitness: Average Evaluation			Fitness: Lowest Evaluation			Fitness: Highest Evaluation			Fitness: Average Evaluation			Fitness: Lowest Evaluation		
Structure	ΔE	Q	F_i	ΔE	Q	F_i	ΔE	Q	F_i	ΔE	Q	F_i	ΔE	Q	F_i	ΔE	Q	F_i
1	1.10	13011.00	11721.60	2.10	13021.00	10761.20	2.20	13022.00	10673.80	1.20	7006.00	6255.36	2.20	14022.00	11493.40	0.00	14000.00	14000.00
2	3.00	12970.00	9976.92	2.10	12979.00	10726.40	1.90	12981.00	10908.40	3.30	13967.00	10501.50	2.60	13974.00	11090.50	3.40	13966.00	10422.40
3	2.10	6489.50	5363.22	1.00	12990.00	11809.10	1.50	12985.00	11291.30	2.80	6986.00	5457.81	2.40	13976.00	11271.00	4.60	13954.00	9557.53
4	0.00	13001.00	13001.00	1.20	13012.00	11617.90	1.20	13012.00	11617.90	0.00	14001.00	14001.00	0.40	13996.00	13457.70	1.60	13984.00	12055.20
5	3.10	6484.50	4950.00	2.70	12973.00	10215.00	3.30	12967.00	9749.62	4.60	6977.00	4778.77	2.80	13972.00	10915.60	5.10	13949.00	9237.75
6	4.00	12960.00	9257.14	4.20	12958.00	9125.35	3.00	12970.00	9976.92	4.60	13954.00	9557.53	4.60	13954.00	9557.53	5.00	13950.00	9300.00
7	2.40	12976.00	10464.50	1.30	12987.00	11492.90	1.90	12981.00	10908.40	3.30	6983.50	5250.75	1.80	13982.00	11849.20	5.00	13950.00	9300.00
8	0.00	13000.00	13000.00	0.50	13005.00	12385.70	0.30	12997.00	12618.40	1.40	6993.00	6134.21	0.40	14004.00	13465.40	1.50	13985.00	12160.90
9	1.50	12985.00	11291.30	0.30	12997.00	12618.40	0.00	13000.00	13000.00	1.10	6994.50	6301.35	0.00	14000.00	14000.00	2.80	13972.00	10915.60
10	0.50	6497.50	6188.10	0.20	13002.00	12747.10	0.50	13005.00	12385.70	0.60	6997.00	6600.94	1.40	14014.00	12293.00	1.30	13987.00	12377.90
mean	1.77	11037.45	9521.38	**1.56**	**12992.40**	**11349.90**	1.58	12992.00	11313.04	2.29	9085.90	7483.92	**1.86**	**13989.40**	**11939.33**	3.03	13969.70	10932.73
stdev	1.38	3137.73	3030.36	1.24	19.00	1150.32	**1.11**	**18.13**	**1093.38**	1.65	3373.14	2940.09	**1.39**	21.25	**1378.44**	1.86	**18.64**	1654.00

	1500nm									1600nm								
	Fitness: Highest Evaluation			Fitness: Average Evaluation			Fitness: Lowest Evaluation			Fitness: Highest Evaluation			Fitness: Average Evaluation			Fitness: Lowest Evaluation		
Structure	ΔE	Q	F_i	ΔE	Q	F_i	ΔE	Q	F_i	ΔE	Q	F_i	ΔE	Q	F_i	ΔE	Q	F_i
1	0.00	15001.00	15001.00	2.00	15020.00	12516.70	2.00	15020.00	12516.70	1.30	8006.50	7085.40	2.40	16024.00	12922.60	0.00	16000.00	16000.00
2	4.70	14953.00	10172.10	3.10	14969.00	11426.70	3.10	14969.00	11426.70	3.90	7980.50	5741.37	3.20	15968.00	12097.00	3.90	15961.00	11482.70
3	4.20	14958.00	10533.80	3.20	14968.00	11339.40	3.20	14968.00	11339.40	3.60	7982.00	5869.12	2.90	15971.00	12380.60	5.30	15947.00	10422.90
4	1.10	7494.50	6751.80	0.20	14998.00	14703.90	0.20	14998.00	14703.90	0.00	16001.00	16001.00	0.70	15993.00	14946.70	1.80	15982.00	13544.10
5	6.00	7470.00	4668.75	4.70	14953.00	10172.10	4.70	14953.00	10172.10	4.60	15954.00	10927.40	3.40	15966.00	11914.90	5.90	15941.00	10025.80
6	6.00	7470.00	4668.75	5.00	14950.00	9966.67	5.00	14950.00	9966.67	6.10	15939.00	9900.00	5.40	15946.00	10354.50	5.80	15942.00	10089.90
7	4.70	14953.00	10172.10	2.60	14974.00	11884.10	2.60	14974.00	11884.10	4.60	7977.00	5463.70	2.20	15978.00	13096.70	5.80	15942.00	10089.90
8	2.70	7486.50	5894.88	0.50	15005.00	14290.50	0.50	15005.00	14290.50	1.30	7993.50	7073.89	0.30	16003.00	15536.90	1.70	15983.00	13660.70
9	2.40	14976.00	12077.40	2.50	14975.00	11980.00	2.50	14975.00	11980.00	1.20	15988.00	14275.00	0.20	15998.00	15684.30	3.30	15967.00	12005.30
10	1.80	14982.00	12696.60	0.40	15004.00	14426.90	0.40	15004.00	14426.90	0.70	8003.50	7479.91	1.50	16015.00	13926.10	1.50	15985.00	13900.00
mean	3.36	11974.40	9263.72	**2.42**	**14981.60**	**12270.70**	**2.42**	**14981.60**	**12270.70**	2.73	11182.50	8981.68	**2.22**	**15986.20**	**13286.03**	3.50	15965.00	12122.13
stdev	2.07	3867.98	3586.51	**1.69**	**23.70**	**1707.37**	**1.69**	**23.70**	**1707.37**	2.07	4120.90	3711.45	**1.62**	24.45	**1727.59**	2.16	**21.64**	2069.68

	1700nm									1800nm								
	Fitness: Highest Evaluation			Fitness: Average Evaluation			Fitness: Lowest Evaluation			Fitness: Highest Evaluation			Fitness: Average Evaluation			Fitness: Lowest Evaluation		
Structure	ΔE	Q	F_i	ΔE	Q	F_i	ΔE	Q	F_i	ΔE	Q	F_i	ΔE	Q	F_i	ΔE	Q	F_i
1	1.90	17019.00	14301.70	0.00	17000.00	17000.00	0.00	17000.00	17000.00	2.00	18020.00	15016.70	0.00	18000.00	18000.00	2.00	18020.00	15016.70
2	4.00	8480.00	6057.14	7.10	16929.00	9900.00	4.30	16957.00	11858.00	4.30	17957.00	12557.30	5.80	17942.00	11355.70	3.90	17961.00	12921.60
3	4.10	16959.00	12027.70	6.40	16936.00	10326.80	5.70	16943.00	10791.70	4.30	8978.50	6278.67	4.60	17954.00	12297.30	3.30	17967.00	13509.00
4	0.70	8496.50	7940.65	0.90	16991.00	15588.10	2.00	16980.00	14150.00	0.70	17993.00	16815.90	1.40	17986.00	15777.20	0.60	18006.00	16986.80
5	5.70	8471.50	5395.86	6.80	16932.00	10078.60	6.30	16937.00	10390.80	6.10	17939.00	11142.20	5.90	17941.00	11283.60	5.70	17943.00	11428.70
6	6.20	16938.00	10455.60	6.20	16938.00	10455.60	6.30	16937.00	10390.80	6.60	17934.00	10803.60	7.20	17928.00	10423.30	5.50	17945.00	11577.40
7	3.50	16965.00	12566.70	5.70	16943.00	10791.70	6.30	16937.00	10390.80	3.70	17963.00	13111.70	5.00	17950.00	11966.70	3.90	17961.00	12921.60
8	0.00	17001.00	17001.00	0.40	16996.00	16342.30	1.90	16981.00	14269.70	0.00	18001.00	18001.00	1.60	17984.00	15503.40	1.50	17985.00	15639.10
9	3.20	16968.00	12854.50	3.70	16963.00	12381.80	3.50	16965.00	12566.70	3.40	17966.00	13407.50	3.70	17963.00	13111.70	1.10	17989.00	16206.30
10	0.00	17000.00	17000.00	0.70	16993.00	15881.30	1.70	16983.00	14515.40	0.00	18000.00	18000.00	2.20	17978.00	14736.10	0.40	17996.00	17303.80
mean	**2.93**	14429.80	11560.09	3.79	**16962.10**	**12874.62**	3.80	16962.00	12632.39	3.11	17075.15	13513.46	3.74	17962.60	13445.50	**2.79**	**17977.30**	**14351.10**
stdev	**2.22**	4103.98	4112.59	2.98	29.82	2963.43	2.32	**23.19**	**2277.23**	2.38	2845.01	3648.87	2.35	**23.48**	2446.59	**1.95**	25.93	**2166.38**

Table 5.8: Structures Fitness for each resonance peak.

	1900nm									2000nm								
	Fitness: Highest Evaluation			Fitness: Average Evaluation			Fitness: Lowest Evaluation			Fitness: Highest Evaluation			Fitness: Average Evaluation			Fitness: Lowest Evaluation		
Structure	ΔE	Q	F_i	ΔE	Q	F_i	ΔE	Q	F_i	ΔE	Q	F_i	ΔE	Q	F_i	ΔE	Q	F_i
1	0.00	19001.00	19001.00	2.00	19020.00	15850.00	0.00	19000.00	19000.00	0.00	20000.00	20000.00	0.00	20000.00	20000.00	0.00	20000.00	20000.00
2	6.50	9467.50	5737.88	4.60	18954.00	12982.20	4.90	18951.00	12718.80	6.80	19932.00	11864.30	6.50	19935.00	12081.80	6.70	19933.00	11935.90
3	6.50	9467.50	5737.88	4.70	18953.00	12893.20	6.50	18935.00	11475.80	5.30	9973.50	6518.63	5.10	19949.00	13211.30	7.20	19928.00	11586.00
4	2.70	9486.50	7469.69	0.80	18992.00	17585.20	2.20	18978.00	15555.70	1.60	19984.00	17227.60	1.60	19984.00	17227.60	1.20	19988.00	17846.40
5	8.20	0.00	0.00	6.60	18934.00	11406.00	7.10	18929.00	11069.60	7.50	19925.00	11385.70	6.60	19934.00	12008.40	7.30	19927.00	11518.50
6	9.00	0.00	0.00	7.10	9464.50	5534.80	7.10	18929.00	11069.60	9.90	0.00	0.00	8.10	19919.00	11005.00	7.50	19925.00	11385.70
7	6.00	18940.00	11837.50	4.00	18960.00	13542.90	7.10	18929.00	11069.60	5.80	19942.00	12621.50	5.60	19944.00	12784.60	7.00	19930.00	11723.50
8	2.00	9490.00	7908.33	0.00	19000.00	19000.00	2.10	18979.00	15685.10	2.50	9987.50	7990.00	1.80	19982.00	16933.90	1.60	19984.00	17227.60
9	5.30	9473.50	6191.83	3.70	18963.00	13841.60	4.00	18960.00	13542.90	3.90	9980.50	7180.22	4.10	19959.00	14155.30	3.30	19967.00	15012.80
10	2.00	9490.00	7908.33	0.10	18999.00	18810.90	1.90	18981.00	15950.40	2.90	9985.50	7740.70	2.50	19975.00	15980.00	2.60	19974.00	15852.40
mean	4.82	9481.60	7179.24	**3.36**	18023.95	**14144.68**	4.29	**18957.10**	13713.75	4.62	13971.00	10252.86	**4.19**	**19958.10**	**14538.79**	4.44	19955.60	14408.88
stdev	2.98	6323.52	5485.47	**2.55**	3007.60	4015.18	2.63	**26.31**	**2733.09**	3.00	6976.05	5706.55	**2.63**	**26.27**	**2882.55**	2.98	29.77	3201.74

Chapter 6

Conclusion and Future works

The process of designing structures in the nanoscale is a challenging task which involves not only setting up the parameters needed to achieve the desired function, but also to plan how to handle problems that may arise from the building process of the nanostructure. For that end, this work is a glimpse at how evolutionary algorithms can be used to design nanostructures, while overcoming the challenges towards quality and robustness of nanometric sized devices. As a sample of that potential, both study cases from this work, had reached results that outperform the bests from literature.

From the photonic crystals cavities optimization, the results obtained in our experiments outnumber those previously presented in the literature by threefold, as shown in section 5.1. Furthermore, the challenge imposed by the computationally expensive experiments in the FDTD simulations could be overcomed by the massivelly distributed genetic algorithm presented in this work.

The presented PCMDGA consists of a single population strategy that distribute evaluations across many different clients on large and heterogeneous computing environments. In this way, the implementation of this algorithm proved to be robust against external issues, such as power shortages and maintenance routines which are common events that disturb algorithms whose the required running time is extensive. Moreover, the results showed that this strategy required less evaluations than previous attempts in literature for solving the same problem.

As computing environments continue to become more distributed and heterogeneous, results from this work show that using an asynchronous strategy for distributed evolutionary algorithms can provide significant benefits in terms of scalability and resilience to heterogeneity and faults.

Simultaneously, to the best of our knowledge, this is the first project proposed to optimize microcavities' structure, mainly focusing on its robustness. Different types of microcavities were optimized and the strategy proposed in this study proved to be effective, leading to structures with higher Quality Factor than those previously described in literature while delivering robustness in the growth process.

Microcavity structures has attracted the attention of scientist and engineers and has been applied to technological or purely scientific purpose. The optimization of microcavities parameters is a challenging task, mainly because some uncertainties are related to the growth process. These cause the synthesis of semiconductor nanodevices with undesirable layers thickness. The optimization procedure proposed here was able to find satisfactory results, overcoming the known experimental solution. Also, the procedure found parameters sets that minimized the problem caused by the uncertainty. The results present high Quality Factor despite the uncertainties involved, which can assist the experts in the development of optimized structures. Many microcavities structures with different resonance peaks were optimized. As expected, the increase in the value of the resonance peak, lead to a higher Quality Factor. In all optimization cases, the shift of the desirable peak position was minimized.

6.1 Future works

From this work, many others may arise. It is possible to highlight:

1. Further investigate on how applying the massivelly distributed genetic algorithm could help improve the results of problems with faster simulations like in the case of optimizing microcavities.

2. Optimize microcavities, taking into account others parameters proposed by experts.

3. Apply neural networks and other surrogate functions for predicting fitness from Photonic Crystals, without actually going through expensive simulations as discussed in [Jin, 2005].

4. Implementing the photonic crystal simulation in a web browser, using novel technologies such as the Native Client [Yee et al., 2009], could lead to a huge leap in distributing the simulations across many clients, since it would be a user friendly way of asking people to help on the optimization process.

5. Optimize Photonic Crystals with PCMDGA taking into account the $\frac{Q}{V}$ ratio, as the fitness value.

6. Optimize structures other than the *L3* cavity and take into account asymmetry using an evolutionary approach.

7. Try others metaheuristics and compare their results with those obtained in this work.

Appendix A

Publications

Published

1. Coelho, F. C. d. S., Melo Mota Costa, A., Paranaiba Vilela Neto, O., and Cotta, E. A. (2013). Microcavities optimization under uncertainty by evolutionary algorithms. In Evolutionary Computation (CEC), 2013 IEEE Congress on, pages 2138–2145. IEEE.

In production

1. Coelho, F. C. d. S., Carneiro, L. S., Cotta, E. A. Paranaiba Vilela Neto, O. (2014). Robustness in microcavities optimization under uncertainty by evolutionary algorithms. Communications in Nonlinear Science and Numerical Simulation, in preparation.

2. Coelho, F. C. d. S., Paranaiba Vilela Neto, O. (2014). A Massively distributed evolutionary approach for semiconductor nanodevices optimization. To be submitted to a conference.

3. Coelho, F. C. d. S., Paranaiba Vilela Neto, O. (2014). Optimizing L3 cavity Photonic Crystal designs with a Massivelly Distributed Genetic Algorithm. To be submitted to a journal.

Appendix B

Microcavities results

B.1 Evolution charts

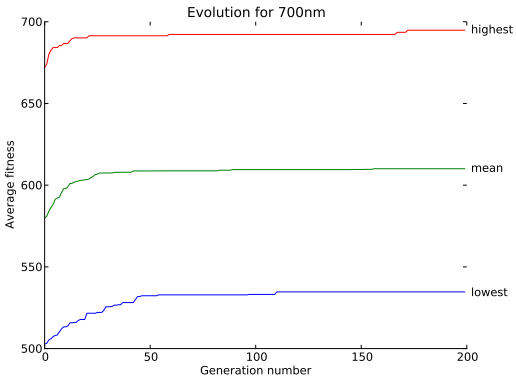

Figure B.1: Evolution for 700nm

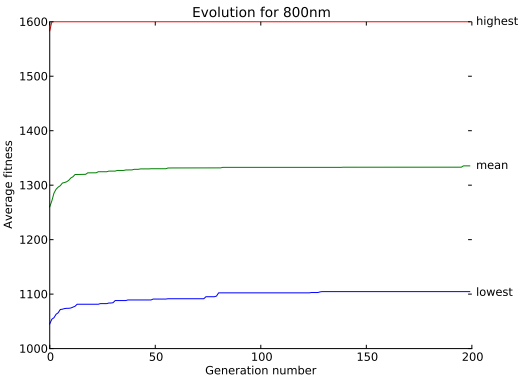

Figure B.2: Evolution for 800nm

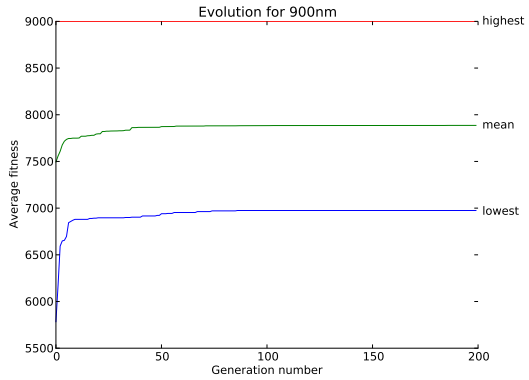

Figure B.3: Evolution for 900nm

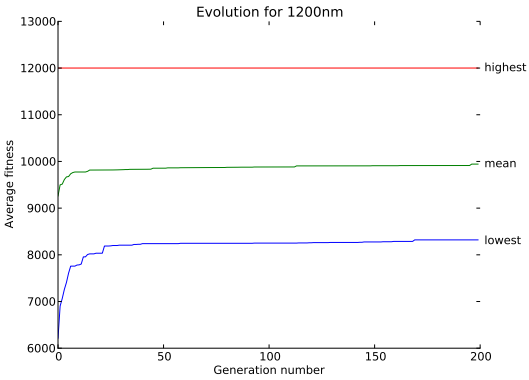

Figure B.6: Evolution for 1200nm

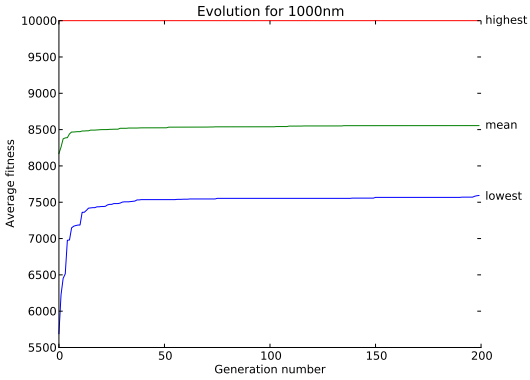

Figure B.4: Evolution for 1000nm

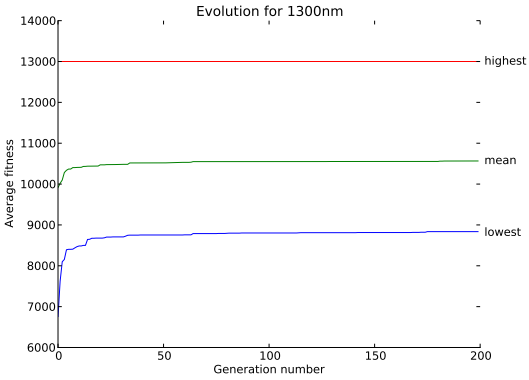

Figure B.7: Evolution for 1300nm

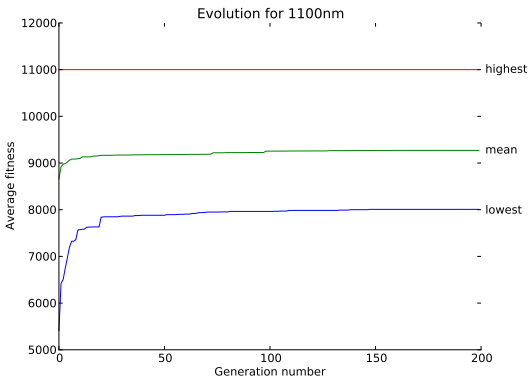

Figure B.5: Evolution for 1100nm

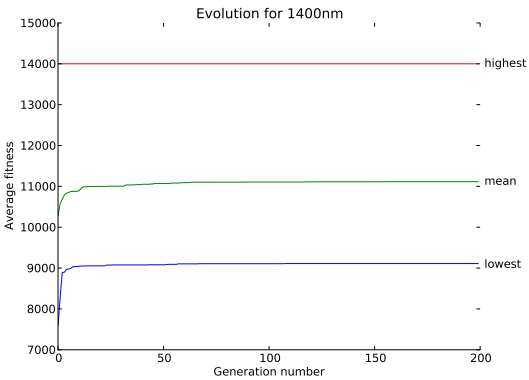

Figure B.8: Evolution for 1400nm

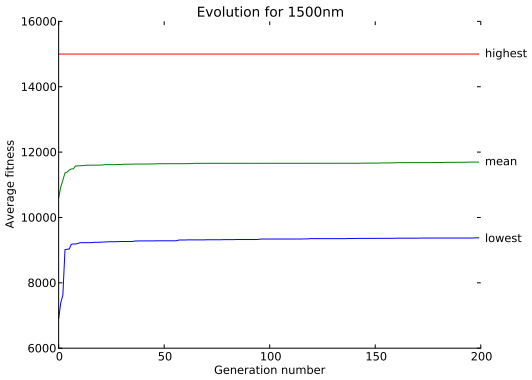

Figure B.9: Evolution for 1500nm

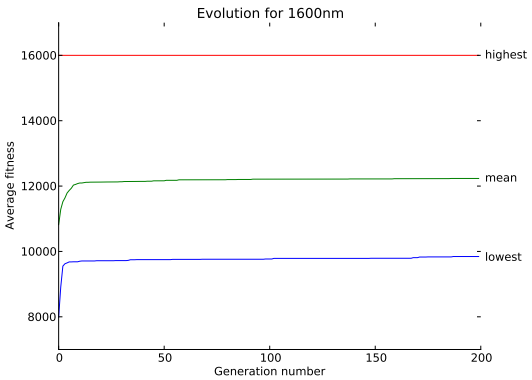

Figure B.10: Evolution for 1600nm

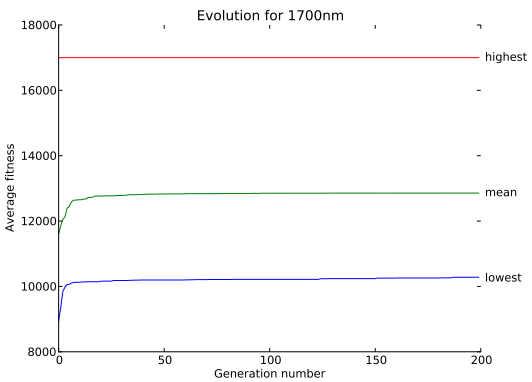

Figure B.11: Evolution for 1700nm

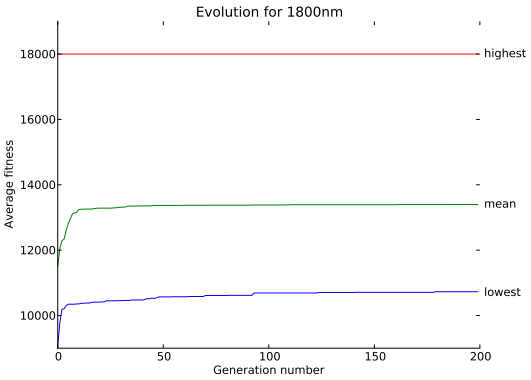

Figure B.12: Evolution for 1800nm

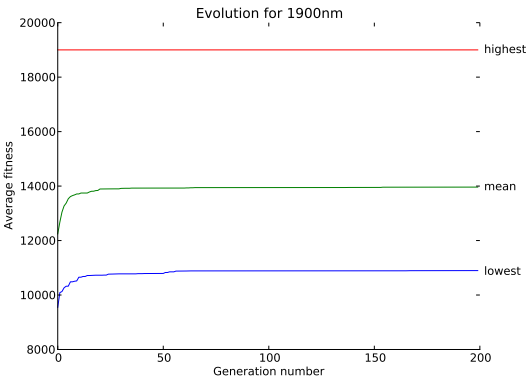

Figure B.13: Evolution for 1900nm

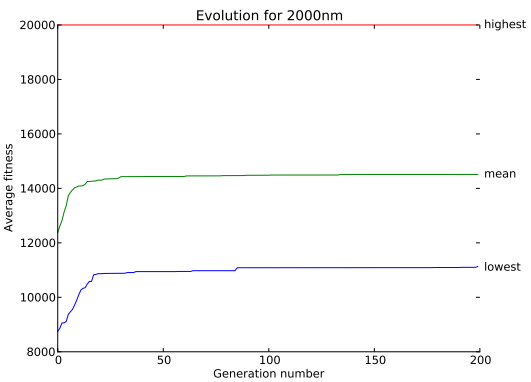

Figure B.14: Evolution for 2000nm

B.2 Reflectances

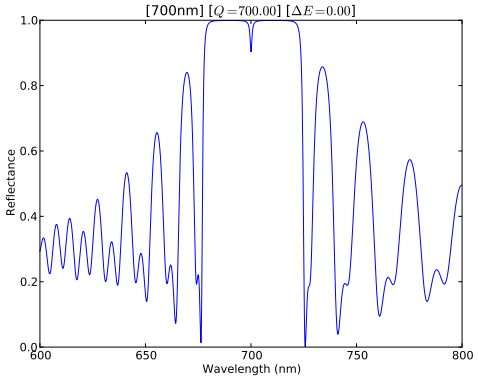

Figure B.15: Reflectance for 700nm

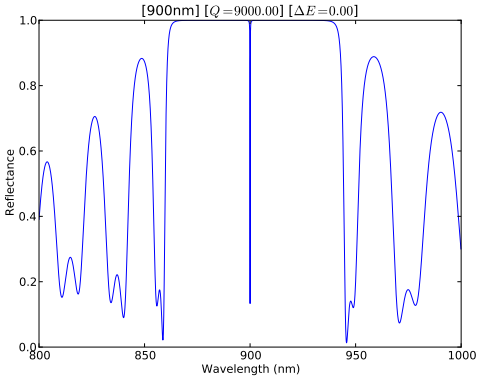

Figure B.17: Reflectance for 900nm

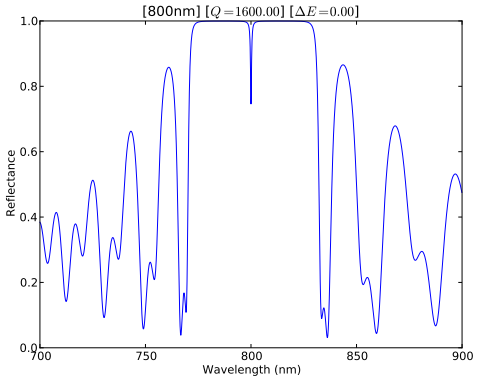

Figure B.16: Reflectance for 800nm

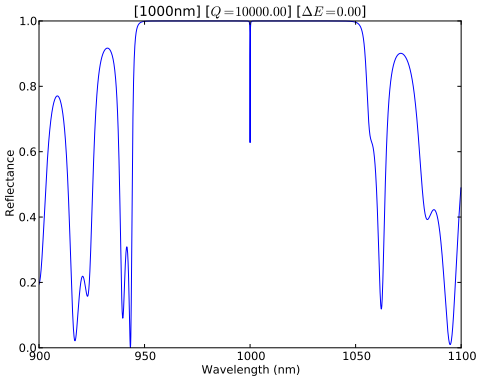

Figure B.18: Reflectance for 1000nm

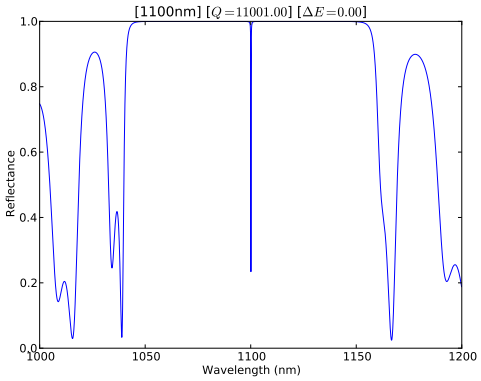

Figure B.19: Reflectance for 1100nm

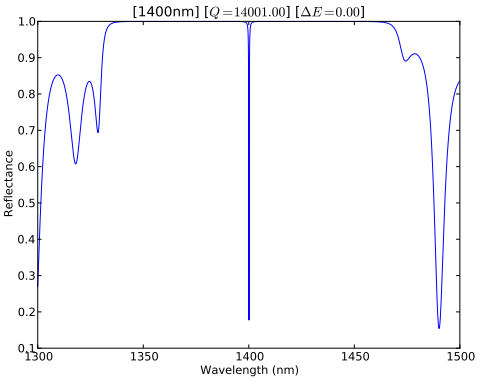

Figure B.22: Reflectance for 1400nm

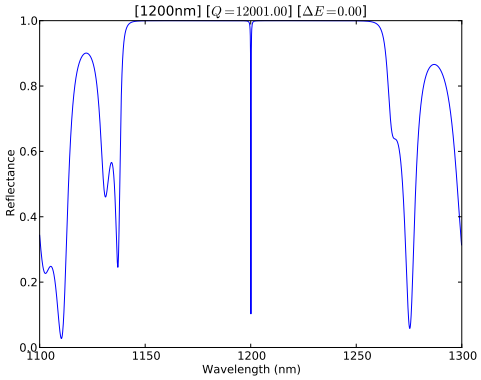

Figure B.20: Reflectance for 1200nm

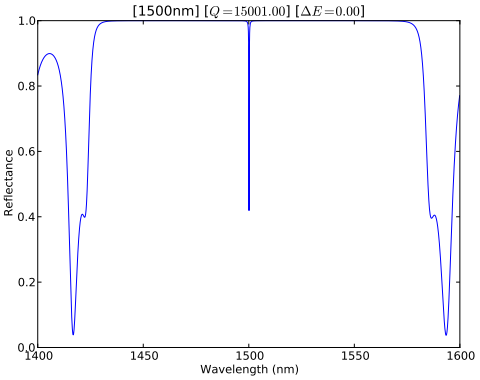

Figure B.23: Reflectance for 1500nm

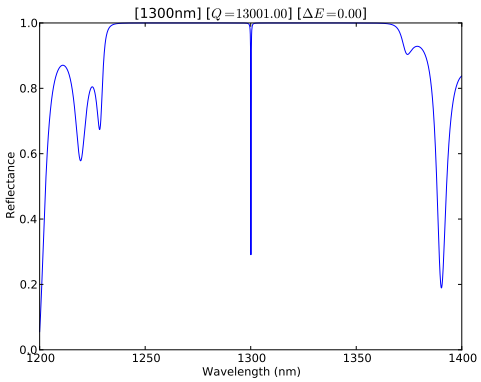

Figure B.21: Reflectance for 1300nm

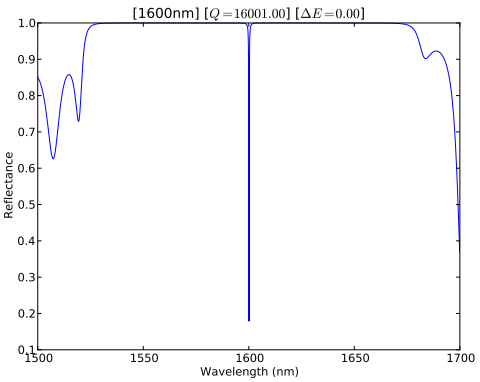

Figure B.24: Reflectance for 1600nm

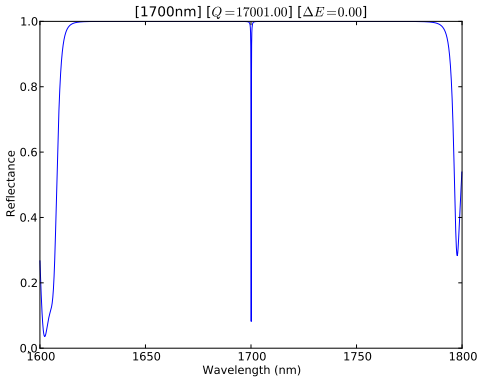

Figure B.25: Reflectance for 1700nm

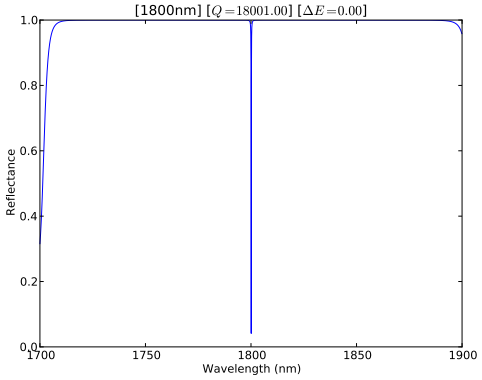

Figure B.26: Reflectance for 1800nm

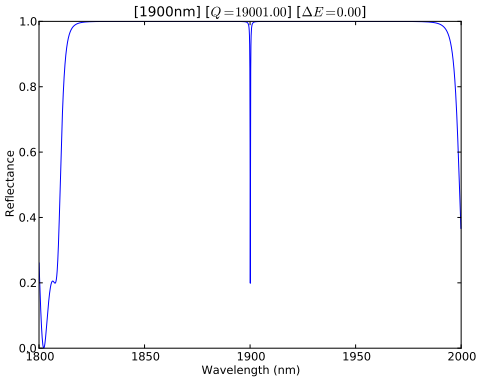

Figure B.27: Reflectance for 1900nm

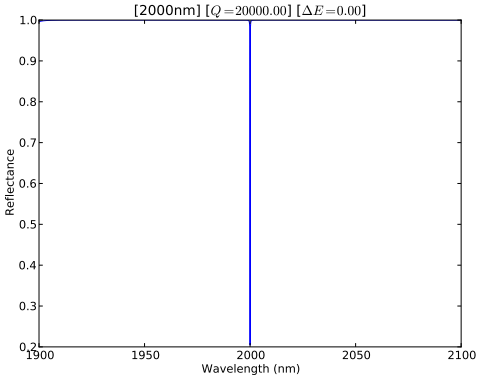

Figure B.28: Reflectance for 2000nm

Bibliography

Akahane, Y., Asano, T., Song, B.-S., and Noda, S. (2003). High-q photonic nanocavity in a two-dimensional photonic crystal. *Nature*, 425(6961):944--947.

Akahane, Y., Asano, T., Song, B.-S., and Noda, S. (2005). Fine-tuned high-q photonic-crystal nanocavity. *Optics express*, 13(4):1202--1214.

Baluja, S. (1992). A massively distributed parallel genetic algorithm. Technical report, DTIC Document.

Banaee, M. and Young, J. F. (2008). Squeezed state generation in photonic crystal microcavities. *Opt. Express*, 16(25):20908--20919.

Berenger, J.-P. (1994). A perfectly matched layer for the absorption of electromagnetic waves. *Journal of computational physics*, 114(2):185--200.

Chalcraft, A., Lam, S., OBrien, D., Krauss, T., Sahin, M., Szymanski, D., Sanvitto, D., Oulton, R., Skolnick, M., Fox, A., et al. (2007). Mode structure of the l3 photonic crystal cavity. *Applied physics letters*, 90(24):241117--241117.

Coelho, F. C. d. S., Melo Mota Costa, A., Paranaiba Vilela Neto, O., and Cotta, E. A. (2013). Microcavities optimization under uncertainty by evolutionary algorithms. In *Evolutionary Computation (CEC), 2013 IEEE Congress on*, pages 2138--2145. IEEE.

Cole, N., Desell, T., González, D. L., de Vega, F. F., Magdon-Ismail, M., Newberg, H., Szymanski, B., and Varela, C. (2010). Evolutionary algorithms on volunteer computing platforms: The milkyway@ home project. In *Parallel and distributed computational intelligence*, pages 63--90. Springer.

Cotta, E. A. (2009). Semiconductor microcavity: An intrinsic optical transistor. *ECS Transactions*, 23(1):545--551.

Cotta, E. A. and Matinaga, F. M. (2007). Bistability double crossing curve effect in a polariton-laser semiconductor microcavity. *arXiv preprint arXiv:0704.2911*.

Croisard, N., Vasile, M., Kemble, S., and Radice, G. (2010). Preliminary space mission design under uncertainty. *Acta Astronautica*, 66(5):654--664.

da Cunha, J. M. (2011). Estudo da nao-linearidade induzida em microcavidades semicondutoras sob a açao de campos elétricos externos. *Universidade Federal do Amazonas*.

De Matos, C., Pugnet, M., and Le Corre, A. (2000). Ultrafast coherent all-optical switching in quantum-well semiconductor microcavity. *Electronics Letters*, 36(1):93--94.

Desell, T., Anderson, D. P., Magdon-Ismail, M., Newberg, H., Szymanski, B. K., and Varela, C. A. (2010). An analysis of massively distributed evolutionary algorithms. In *Evolutionary Computation (CEC), 2010 IEEE Congress on*, pages 1--8. IEEE.

Fan, W., Hao, Z., Stock, E., Kang, J., Luo, Y., and Bimberg, D. (2011). Comparison between two types of photonic-crystal cavities for single-photon emitters. *Semiconductor Science and Technology*, 26(1):014014.

Giannakoglou, K. (2002). Design of optimal aerodynamic shapes using stochastic optimization methods and computational intelligence. *Progress in Aerospace Sciences*, 38(1):43--76.

Goh, C.-K. and Tenne, Y. (2010). *Computational intelligence in expensive optimization problems*, volume 2. Springer.

Håkansson, A., Sanchis, P., Sánchez-Dehesa, J., and Martí, J. (2005). High-efficiency defect-based photonic-crystal tapers designed by a genetic algorithm. *Journal of Lightwave Technology*, 23(11):3881.

Imamōglu, A. and Ram, R. (1994). Semiconductor lasers without population inversion. *Optics letters*, 19(21):1744--1746.

Jiang, J., Cai, J., Nordin, G. P., and Li, L. (2003). Parallel microgenetic algorithm design for photonic crystal and waveguide structures. *Optics letters*, 28(23):2381--2383.

Jin, Y. (2005). A comprehensive survey of fitness approximation in evolutionary computation. *Soft computing*, 9(1):3--12.

Joannopoulos, J. D., Johnson, S. G., Winn, J. N., and Meade, R. D. (2011). *Photonic crystals: molding the flow of light*. Princeton university press.

Kasprzak, J., Richard, M., Kundermann, S., Baas, A., Jeambrun, P., Keeling, J., FM Marchetti, M., et al. (2006). Bose–einstein condensation of exciton polaritons. *Nature*, 443(7110):409--414.

Laredo, J. L. J., Eiben, A., van Steen, M., and Merelo, J. J. (2010). Evag: a scalable peer-to-peer evolutionary algorithm. *Genetic Programming and Evolvable Machines*, 11(2):227--246.

Ma, L., Rakher, M. T., Stevens, M. J., Slattery, O., Srinivasan, K., and Tang, X. (2011). Temporal correlation of photons following frequency up-conversion. *Optics express*, 19(11):10501--10510.

Michalewicz, Z. (1996). *Genetic algorithms+ data structures= evolution programs*. springer.

Michler, P., Kiraz, A., Becher, C., Schoenfeld, W., Petroff, P., Zhang, L., Hu, E., and Imamoglu, A. (2000). A quantum dot single-photon turnstile device. *Science*, 290(5500):2282--2285.

Morin, S. E., Wu, Q., and Mossberg, T. W. (1992). Cavity quantum electrodynamics at optical frequencies. *Optics and Photonics News*, 3(8):8--14.

Noshad, M., Abbasi, A., Ranjbar, R., and Kheradmand, R. (2012). Novel all-optical logic gates based on photonic crystal structure. In *Journal of Physics: Conference Series*, volume 350, page 012007. IOP Publishing.

Oskooi, A. F., Roundy, D., Ibanescu, M., Bermel, P., Joannopoulos, J. D., and Johnson, S. G. (2010). Meep: A flexible free-software package for electromagnetic simulations by the fdtd method. *Computer Physics Communications*, 181(3):687--702.

Pablo Vasco Cano, J. (2013). *Reflectivity calculations in L3 Photonic Crystal slab cavities*. Universidade Federal de Minas Gerais.

Paladini, V., Donateo, T., de Risi, A., and Laforgia, D. (2007). Super-capacitors fuel-cell hybrid electric vehicle optimization and control strategy development. *Energy Conversion and Management*, 48(11):3001--3008.

Quan, Q., Deotare, P. B., and Loncar, M. (2010). Photonic crystal nanobeam cavity strongly coupled to the feeding waveguide. *Applied Physics Letters*, 96(20):203102--203102.

Quan, Q. and Loncar, M. (2011). Deterministic design of wavelength scale, ultra-high q photonic crystal nanobeam cavities. *arXiv preprint arXiv:1108.2675*.

Raimond, J.-M., Brune, M., and Haroche, S. (2001). Manipulating quantum entanglement with atoms and photons in a cavity. *Reviews of Modern Physics*, 73(3):565.

Rezende, S. M. (2004). *Materiais e dispositivos eletrônicos*. Livraria da Física.

Sanchis, L., Hakansson, A., López-Zanón, D., Bravo-Abad, J., and Sánchez-Dehesa, J. (2004). Integrated optical devices design by genetic algorithm. *Applied Physics Letters*, 84(22):4460--4462.

Saucer, T. W. and Sih, V. (2013). Optimizing nanophotonic cavity designs with the gravitational search algorithm. *Optics express*, 21(18):20831--20836.

Scherer, A., Loncar, M., et al. (2006). Photonic crystal laser sources for chemical detection. US Patent 7,079,240.

Tantar, A.-A., Melab, N., and Talbi, E.-G. (2008). A grid-based genetic algorithm combined with an adaptive simulated annealing for protein structure prediction. *Soft Computing*, 12(12):1185--1198.

Vučković, J., Lončar, M., Mabuchi, H., and Scherer, A. (2001). Design of photonic crystal microcavities for cavity qed. *Physical Review E*, 65(1):016608.

Ye, Z., Shen, L., and He, S. (2004). Design for 2d anisotropic photonic crystal with large absolute band gaps by using a genetic algorithm. *The European Physical Journal B-Condensed Matter and Complex Systems*, 37(4):417--419.

Yee, B., Sehr, D., Dardyk, G., Chen, J. B., Muth, R., Ormandy, T., Okasaka, S., Narula, N., and Fullagar, N. (2009). Native client: A sandbox for portable, untrusted x86 native code. In *Security and Privacy, 2009 30th IEEE Symposium on*, pages 79--93. IEEE.